

Evidence that GCN1 and GCN20, Translational Regulators of GCN4, Function on Elongating Ribosomes in Activation of eIF2 α Kinase GCN2

MATTHEW J. MARTON,¹† CARLOS R. VAZQUEZ DE ALDANA,¹‡ HONGFANG QIU,¹
KALPANA CHAKRABURTTY,² AND ALAN G. HINNEBUSCH^{1*}

Laboratory of Eukaryotic Gene Regulation, National Institute of Child Health and Human Development, Bethesda, Maryland 20892,¹ and Department of Biochemistry, Medical College of Wisconsin, Milwaukee, Wisconsin 53226²

Received 14 February 1997/Returned for modification 7 April 1997/Accepted 14 May 1997

In the yeast *Saccharomyces cerevisiae*, phosphorylation of translation initiation factor eIF2 by protein kinase GCN2 leads to increased translation of the transcriptional activator GCN4 in amino acid-starved cells. The GCN1 and GCN20 proteins are components of a protein complex required for the stimulation of GCN2 kinase activity under starvation conditions. GCN20 is a member of the ATP-binding cassette (ABC) family, most of the members of which function as membrane-bound transporters, raising the possibility that the GCN1/GCN20 complex regulates GCN2 indirectly as an amino acid transporter. At odds with this idea, indirect immunofluorescence revealed cytoplasmic localization of GCN1 and no obvious association with plasma or vacuolar membranes. In addition, a fraction of GCN1 and GCN20 cosedimented with polysomes and 80S ribosomes, and the ribosome association of GCN20 was largely dependent on GCN1. The C-terminal 84% of GCN20 containing the ABCs was found to be dispensable for complex formation with GCN1 and for the stimulation of GCN2 kinase function. Because ABCs provide the energy-coupling mechanism for ABC transporters, these results also contradict the idea that GCN20 regulates GCN2 as an amino acid transporter. The N-terminal 15 to 25% of GCN20, which is critically required for its regulatory function, was found to interact with an internal segment of GCN1 similar in sequence to translation elongation factor 3 (EF3). Based on these findings, we propose that GCN1 performs an EF3-related function in facilitating the activation of GCN2 by uncharged tRNA on translating ribosomes. The physical interaction between GCN20 and the EF3-like domain in GCN1 could allow for modulation of GCN1 activity, and the ABC domains in GCN20 may be involved in this regulatory function. A human homolog of GCN1 has been identified, and the portion of this protein most highly conserved with yeast GCN1 has sequence similarity to EF3. Thus, similar mechanisms for the detection of uncharged tRNA on translating ribosomes may operate in yeast and human cells.

In the yeast *Saccharomyces cerevisiae*, starvation for an amino acid or a defective aminoacyl-tRNA synthetase triggers increased transcription of over 40 genes encoding enzymes involved in amino acid biosynthesis. This response, known as general amino acid control, requires derepression of GCN4, a transcriptional activator which binds to the promoter regions of genes subject to the general control. *GCN4* expression is increased at the translational level by a regulatory mechanism involving phosphorylation of translation initiation factor eIF2 by the protein kinase GCN2 (24). During the process of initiation, eIF2 delivers the initiator methionyl-tRNA (tRNA_i^{Met}) to 40S ribosomal subunits in an eIF2/GTP/Met-tRNA_i^{Met} ternary complex and is released as an eIF2/GDP binary complex. eIF2 must be recycled to the GTP-bound state that is competent for ternary complex formation by the guanine nucleotide exchange factor eIF2B (22). Phosphorylation of the alpha subunit of eIF2 (eIF2 α) by GCN2 converts eIF2 from a substrate to an inhibitor of eIF2B, lowering the concentration of ternary complexes in the cell. This depletion of ternary complexes

stimulates translation of *GCN4* mRNA because of four short upstream open reading frames (uORFs) in its leader sequence. In cells containing abundant amino acids, the uORFs block the flow of scanning ribosomes to the *GCN4* initiation codon. In starved cells, the reduction in ternary complexes brought about by phosphorylation of eIF2 allows ribosomes to bypass the uORFs and initiate translation at the *GCN4* start codon (24).

It has been proposed that GCN2 is activated in amino acid-starved cells by direct binding of uncharged tRNA to a regulatory region located C terminal to the kinase domain with sequence similarity to histidyl-tRNA synthetases (48). In accordance with this hypothesis, the synthetase-related domain in GCN2 binds tRNAs in vitro in a manner dependent on sequence motifs characteristic of class II aminoacyl-tRNA synthetases, and these conserved sequences in GCN2 are required for its regulatory function in vivo (49). A fraction of GCN2 is found associated with ribosomal subunits and polysomes in cell extracts and its ability to interact with ribosomes requires the extreme C-terminal segment of the protein, another domain essential for *GCN2* function in vivo. Based on these last results, it was suggested that GCN2 would be stimulated by uncharged tRNAs only when it is bound to translating ribosomes (35).

The *GCN1*- and *GCN20*-encoded proteins are additionally required for activation of GCN2 in starved cells. Mutations affecting these proteins reduce (*GCN20*) or abolish (*GCN1*) eIF2 α phosphorylation by GCN2; consequently, they impair cell growth on media containing inhibitors of amino acid bio-

* Corresponding author. Phone: (301) 496-4480. Fax: (301) 496-6828.

† Present address: The Seattle Project, Program in Molecular Pharmacology, Fred Hutchinson Cancer Research Center, Seattle, WA 98104.

‡ Present address: Departamento de Microbiología y Genética, CSIC/Universidad de Salamanca, Salamanca, Spain.

synthesis and suppress the growth-inhibitory effects of mutationally activated forms of GCN2. Inactivating GCN1 or GCN20 has no effect on eIF2 α phosphorylation in yeast cells expressing the human eIF2 α kinase PKR in place of GCN2 (31, 47). Neither *gcn1* nor *gcn20* mutations reduce GCN2 expression, nor do they decrease GCN2 kinase activity in immune-complex assays (31, 47). Based on these findings, it was proposed that GCN1 and GCN20 mediate the activation of GCN2 kinase function by uncharged tRNA in amino acid-starved cells. GCN1 and GCN20 were found associated with one another in vivo; however, no evidence was obtained for physical interactions between these proteins and GCN2 (47).

GCN20 is an 85-kDa protein that contains two regions highly related to the nucleotide-binding domains in proteins belonging to the ATP-binding cassette (ABC) superfamily of proteins (47). With few exceptions, ABC proteins are membrane-bound transporters which couple the energy of ATP hydrolysis to the transport of substrates against a concentration gradient. In every known case, the transporter consists of (i) two ca. 200-amino-acid cassettes containing the Walker A and B motifs for ATP binding and (ii) two hydrophobic domains, each capable of spanning a membrane six times. The four domains appear to be modular in function, as they can be expressed as four individual polypeptides, as two-domain proteins containing either two ABC cassettes, two transmembrane domains, or one of each type of domain, or with all four domains fused in a single polypeptide (15, 23).

Considering that GCN20 is a member of the ABC protein superfamily, and that GCN1 is a large (297-kDa) protein with multiple segments sufficiently hydrophobic to function as membrane-spanning domains (MSDs) (31), it seemed possible that GCN1 and GCN20 constitute an ABC transporter that indirectly stimulates GCN2 kinase activity in amino acid-deprived cells. Since uncharged tRNA appears to be the activating ligand for GCN2 (29, 49), the putative GCN1/GCN20 transporter would have to promote accumulation of uncharged tRNA under amino acid starvation conditions. One way to satisfy this condition would be to postulate that GCN1 and GCN20 function by transporting amino acids from the cytoplasm to the vacuole, where large pools of amino acids are stored in yeast (51). In their absence, the cytoplasmic concentrations of amino acids (and charged tRNAs) would remain high even when an amino acid biosynthetic pathway was inhibited by an amount that normally triggers derepression of *GCN4*. GCN2 would not be activated until the vacuolar pools were depleted, at which point protein synthesis would be completely impaired. Several vacuolar amino acid transport activities (27, 40, 41) and a vacuolar ABC transporter (*YCF1*) (44, 50) have been found in yeast.

Except for a predicted protein of unknown function (encoded by ORF YER036c), the ABC domains in GCN20 are more similar to those present in translation elongation factor 3 (EF3) and its two close relatives (ORF YNL014w and ORF YPL226w) than it is to any other ABC proteins in *S. cerevisiae* (47). EF3 is one of the few ABC proteins apparently not involved in membrane transport. It is a 116-kDa protein (39) with ribosome-dependent ATPase and GTPase activities required for translation elongation by yeast ribosomes in vitro (10, 43). Biochemical studies indicate that EF3 stimulates binding of the EF1 α /GTP/aminoacyl-tRNA ternary complex to the A (aminoacyl) site of the ribosome by facilitating release of the deacylated tRNA from the ribosomal E (exit) site (45). In addition, EF3 appears to affect translational fidelity because strains overexpressing EF3 are hypersensitive to aminoglycoside antibiotics and purified EF3 can stimulate binding of cog-

nate tRNAs at the expense of noncognate tRNAs to the ribosome (25, 39, 46).

Interestingly, GCN1 is also similar to EF3 in the region N terminal to the ABCs in EF3; however, GCN1 does not contain the conserved ATP-binding cassettes of ABC proteins (31). Besides the two close relatives of EF3, GCN1 is the only yeast protein that shows strong similarity to this portion of EF3. The sequence similarity to EF3 shown by GCN1 and GCN20 suggested an alternative hypothesis for their role in stimulating *GCN4* translation, wherein they function on the ribosome to mediate activation of GCN2 by uncharged tRNA. More specifically, GCN1 and GCN20 could be needed to bind uncharged tRNA to the ribosomal A site or deliver it to the HisRS-related domain in GCN2 for kinase activation. Such an activity might be related to the proposed role of EF3 in stimulating release of deacylated tRNAs from the E site or in the selection of cognate tRNAs at the A site.

We set out to distinguish between these two hypotheses, and in this report, we present several lines of evidence more consistent with the idea that GCN1 and GCN20 function on ribosomes in regulating GCN2. We found that GCN1 is located throughout the cytoplasm and that both GCN1 and GCN20 can stably interact with translating 80S ribosomes. In addition, the C-terminal 84% of GCN20 containing the ABCs was found to be dispensable for its regulatory function in stimulating *GCN4* translation. These results contradict a role for GCN20 in transport of amino acids and suggest that GCN1 and GCN20 function on ribosomes. The critical N-terminal segment of GCN20 was found to interact specifically with the most EF3-like segment of GCN1; in addition, the EF3-like domain in GCN1 was found to be highly conserved in a human homolog of GCN1. These results establish the functional significance of the EF3-like domain in GCN1, and they support the notion that GCN1 performs an EF3-related function on the ribosome in regulating GCN2 kinase activity.

MATERIALS AND METHODS

Plasmids. Plasmid p1413 (formerly pLC13), containing the *GCN1* gene on an 8.7-kb insert in plasmid pRS316 (42), was previously described (31, 47). The c-Myc epitope LEEOKLISEEDLLRKR was placed at the C terminus of GCN1 in three steps. First, plasmid p1829 was constructed by digesting plasmid p1413 with *NotI*, creating blunt ends with the Klenow fragment, and religating to destroy the *NotI* site in the polylinker and create the *NgoMI* site necessary to construct plasmid p2352 (see below). A new *NotI* site was introduced immediately preceding the termination codon by using PCR and primers MJM20 (see Table 1 for the sequences of all oligonucleotides used in this study) and pLCKpnI to amplify the 3' end of the gene and incorporate the new restriction site. The PCR amplification product was digested with *PacI* and *BstEII* and subcloned into similarly digested plasmid p1829, creating plasmid p1830. The *NotI* site adds three alanine residues to the C terminus of GCN1. Oligonucleotides MJM23 and its complement MJM24, which encode the c-Myc epitope between two *NotI* restriction sites, were hybridized, digested with *NotI*, and ligated to *NotI*-digested plasmid p1830 to form plasmid p1831.

The *gcn1- Δ 1* allele (deletion of coding sequences N terminal to the *PfI*MI site) was constructed by PCR amplification of the promoter region and 5' end of *GCN1*, using the M13-20 sequencing primer and MJM51, which introduces *NheI* and *PfI*MI sites immediately downstream of the *GCN1* initiator codon. The *NgoMI*- and *PfI*MI-digested PCR product was cloned into similarly digested plasmid p1831 to create plasmid p2352. The *gcn1- Δ 2* allele (the *PfI*MI-to-*NheI* internal deletion) was constructed by digesting plasmid p1831 with *PfI*MI, treating with T4 DNA polymerase to remove the 3' overhang, and then digesting with *NheI* and incubating with T4 DNA polymerase to fill in the 5' overhang. The resulting blunt-ended fragment was religated to form plasmid p2353. The *gcn1- Δ 3* allele (the *NheI*-to-*MluI* internal deletion) was constructed by digesting p1831 with *NheI* and *MluI*, creating blunt ends with T4 DNA polymerase, and religating to form plasmid p2354.

The *gcn1- Δ 4* and *gcn1- Δ 5* alleles (the *MluI*-to-*XhoI* and *XhoI*-to-*BstXI* internal deletions, respectively) were constructed in several steps. First, the *XcmI* site of plasmid pRS316 was destroyed by fusion PCRs in which oligonucleotide pairs MJM40/MJM41 and MJM42/MJM43 were amplified with AmpliTaq (Perkin-Elmer), using plasmid pRS316 as the template. The resulting PCR products were combined, mixed with outside primers MJM40 and MJM43, and reamplified.

TABLE 1. Oligonucleotides used

Name	Sequence ^a
MJM20.....	5' GAACTGAGTGA ^{CTT} GTCTC 3'
MJM23.....	5' GGAAAAAGCGGCCGCATTGGAAGAACAAA AGTTGATTTCTGAAGAAGACTTGTGAGAAA GAGAGCGGCCGCAAAAGGAA 3'
MJM24.....	Complementary to MJM23
MJM28.....	5' CAAAAGTCGACTTAAGCTTGAGCAGAACCG AG 3'
MJM33.....	5' GCAAAAAGCCATGGAGGCCGGTGATTACTT GGGTATC 3'
MJM40.....	5' TCTCCGAACAGAAGGAAGAAC 3'
MJM41.....	5' TAATGCTTCAACTA ^{CT} CCAGTAATTCCTTCG TGGTACGACA 3'
MJM42.....	5' TTGTGTGCTTCATTGGATGTTCTGACCACGA AGGAATTA ^{CT} TGG 3'
MJM43.....	5' TGCTTCAAACCGCTAACAATAC 3'
MJM45.....	5' GGCTTGAGATTATTGCG 3'
MJM46.....	5' TATGCGCCATTATAGCCTTAGTGGCTCGAGC GGTTGCATCTCAACTTC 3'
MJM47.....	5' GAAGTTAGAGATGCAACCGCTCGAGCCACTA AGGCTATAATGGCCGATA 3'
MJM48.....	5' GCGGCTAAAATTCTATCAC 3'
MJM51.....	5' TTCTTTACCAAAATATATGGGCTAGCTGTCATC ACTGTAGGA 3'
MJM52.....	5' CGCGTCCGCTAGCGCGCC 3'
MJM53.....	5' TCGAGGCGCGCTAGCGGA 3'
MJM54.....	5' TCGAGGCTCAGCGAACGCGTCCGTTA 3'
MJM55.....	5' GGACGCGTTCGCTGAGCC 3'
MJM56.....	5' GCAACGCGTCCACCGGT 3'
MJM57.....	5' TGAACCGGTGGACGCGTGTCTAAC 3'
MJM58.....	5' TCAGCCCAAGTTACTGGTA 3'
MJM59.....	5' CCGGTACCAGTAACTGGGC 3'
MJM85.....	5' CAACCGATTCCAACCTAACGGGACTTC 3'
MJM89.....	5' CATTGCCCAAGAAGCTCCACTGACC 3'
O103.....	5' AAAGATCTGGTTGACAGATAAGGCTCTTGC CAAGGACAATCTCATTCTCCAATCACC GGAA AAGG 3'
O105.....	5' TTATTATCCGGT ^{AT} CAAAAATCTCGTGTA 3'
O106.....	5' TACACGAGATTTT ^{AT} CACCGGATAATAA 3'
AP1.....	5' CCATCCTAATCAGACTCACTATAGGGC 3'
M13-20.....	5' GTAAACAGACGCCAGT 3'

^a The underlining in MJM23 denotes *NotI* sites flanking the coding sequences for the c-Myc-epitope; in O103, O105, and O106, underlining denotes the changes achieved by site-directed mutagenesis.

The final PCR product was digested with *NcoI* and *NdeI* and ligated to similarly digested plasmid pRS316, forming plasmid p2370. The *Ngo*M1-to-*SalI* fragment of plasmid p1831 was subcloned into similarly digested plasmid p2370, creating plasmid p2372. This plasmid was then digested with *XhoI*, treated with Klenow fragment to create blunt ends, and religated, forming plasmid p2373. Second, an *XhoI* site was engineered into the *GCN1* coding sequence by making a silent T-to-A substitution at nucleotide 4293 (numbered according to reference 31) as follows. The *XhoI* site was created by fusion PCR using primer pairs MJM45/MJM46 and MJM47/MJM48 and p1831 as the template for the first amplification and primers MJM45 and MJM48 for the second amplification. The resulting PCR product was digested with *MluI* and *BstXI* and ligated to similarly digested plasmid p2373, forming plasmid p2367. Finally, to create the *gcn1-Δ4* allele (*MluI*-to-*XhoI* internal deletion), oligonucleotides MJM52 and MJM53 were hybridized and ligated to *MluI*- and *XhoI*-digested plasmid p2367, forming plasmid p2355. The *gcn1-Δ5* allele (the *XhoI*-to-*BstXI* internal deletion) was constructed by hybridizing oligonucleotides MJM54 and MJM55 and ligating them to *XhoI*- and *BstXI*-digested plasmid p2367, forming plasmid p2356.

The *gcn1-Δ6* allele (the *BstXI*-to-*BlpI* internal deletion) was constructed by annealing oligonucleotides MJM56 and MJM57 and ligating them to *BstXI*- and *BlpI*-digested plasmid p1831, forming plasmid p2357. The *gcn1-Δ7* allele (the *BlpI*-to-*AgeI* internal deletion) was constructed by annealing oligonucleotides MJM58 and MJM59 and ligating to *BlpI*- and *AgeI*-digested plasmid p1831. The *gcn1-Δ9* allele (deletion of the N-terminal coding sequences to the *NheI* site) was constructed by digesting plasmid p2352 with *NheI* and religating, forming plasmid p2362. The *gcn1-Δ10* (the *MluI*-to-*BlpI* internal deletion) was constructed by digesting plasmid p1831 with *MluI* and *BlpI*, creating blunt ends with T4 DNA polymerase, and religating to form plasmid p2363. The *gcn1-Δ11* and *gcn1-Δ12*

alleles (the *HpaI* internal deletion and the *BclI* internal deletion, respectively) were constructed by digesting plasmid p1831 with either *HpaI* or *BclI* and religating to form plasmids p2364 and p2365, respectively. The *gcn1-Δ13* allele (the *BspEI* internal deletion) was constructed by digesting plasmid p1831 with *BspEI*, creating blunt ends with T4 DNA polymerase, and religating to form plasmid p2366. The sequences of all junctions of internal deletion alleles were confirmed by the dideoxy-chain termination method using a Sequenase 2.0 kit (U.S. Biochemical Corp.).

The two-hybrid vectors encoding the GAL4 DNA-binding domain (pAS1-CYH2) and GAL4 activation domain (pACT II) have been previously described (14). Plasmid p1809, containing the C-terminal two-thirds of GCN1 (residues 672 to 2672) fused to the GAL4 DNA-binding domain in pAS1-CYH2, and plasmid p1825, containing the first 118 residues of GCN20 fused to the GAL4 activation domain, also have been described (47). Plasmid p1816 was constructed by digesting plasmid p1809 with *CeII* and *BstEII* (located 15 bp downstream of the *GCN1* termination codon), creating blunt ends with the Klenow fragment, and religating. Plasmid p1817 was constructed by PCR amplification of the EF3-like region of GCN1 by using primers MJM28 and MJM33, which incorporated *SfiI* and *SalI* restriction sites at the 5' and 3' ends of the PCR product, respectively. The amplified product and the two-hybrid vector pAS1-CYH2 were digested with *SfiI* and *SalI* and ligated to form plasmid p1817. Plasmid p2369 was constructed by digesting plasmid p1817 with *BamHI* and *SalI*, forming blunt ends with the Klenow fragment, and religating.

Plasmid p1867, containing a *GCN20* allele with novel *BamHI* and *HindIII* sites located, respectively, upstream and downstream of the coding sequence, and p1868, containing a frameshift after codon 117, were described previously (47). Plasmid p2485, bearing the *GCN20* allele with an *SphI* site inserted after the second codon, was constructed by replacing the *BamHI*-*HindIII* fragment of p1867 with a PCR-derived fragment that changed the sequence from ATG GCA AGC ATC GGT TCG to ATG GCA AGC ATG CGT (the *SphI* site is underlined). Plasmid p2486 was derived from plasmid p2485 by digestion with *SphI* and recircularization of the resulting product, removing codons 4 to 118. Plasmid p2489, which contains an internal deletion that removes codons 97 to 117, was constructed by PCR amplifying the region from -161 to +288 (numbered relative to the ATG codon) with oligonucleotides that added *NotI* and *SphI* sites to the ends of the fragment and inserting it between these two sites in plasmid p2486. Plasmids p1728 and p1729 containing wild-type *GCN20* in pRS316 were described previously (47). Plasmids p1738, p1739, and p1740 were constructed by digesting p1729 with *Clal* and *SnaBI*, *Clal* and *EcoRI*, *Clal* and *SphI*, respectively, filling in the ends with T4 DNA polymerase, and religating the products. (The *Clal* site just mentioned is in the polylinker.)

Plasmids p1922 and p1924, containing, respectively, codons 1 to 3 and 1 to 457 of *GCN20* fused to *lacZ*, were described previously (47). Plasmids p2487, p2488, and Jp233 contain *GCN20-lacZ* alleles in which *lacZ* is fused to codons 118, 96, and 187, respectively, of *GCN20*. To construct p2487, the *SphI* site in *GCN20* was replaced with *BamHI* and *SalI* sites by site-directed mutagenesis, yielding plasmid p2541. A *BamHI* fragment containing *lacZ* isolated from pR111 (38) was inserted at the *BamHI* site in p2541, and the resulting plasmid was digested with *SalI* to remove *GCN20* amino acids 119 to 752. To construct p2488, the *GCN20* sequence from -161 to +287 was PCR amplified by using oligonucleotide primers that added *XbaI* and *BamHI* sites to the ends of the fragment, which was inserted between the corresponding sites in p1633 (47). To construct Jp233, the sequence from -161 to +560 was PCR amplified by using oligonucleotide primers that added *XbaI* and *NotI* sites to the ends of the fragment, which was inserted between the corresponding sites in p1633. Plasmids Jp237 and p2491 contain the *GCN20-lacZ* allele with *lacZ* fused to codon 457 of *GCN20* but with internal deletions of codons 4 to 118 and 97 to 117, respectively. To construct Jp237 and p2491, the *NotI*-*SphI* fragments from p2486 and p2489, respectively were inserted into the corresponding sites in p1924.

Plasmid p2340, encoding wild-type *GCN20* tagged with the FLAG epitope at its C terminus, was constructed by inserting the *SacI*-*HindIII* fragment isolated from plasmid p1870 (47) at the corresponding sites of the *LEU2* centromeric vector YClac111 (20). Plasmid p2343, containing the *GCN20-G371D*, *G654D* allele, was constructed in several steps. The PCR was performed with the mutagenic primer O103 to introduce the G371D mutation into the *SphI*-*BglII* fragment, which was then inserted into plasmid p1729 (47) to produce plasmid Jp259. The G654D mutation was introduced into a *SnaBI*-*HindIII* fragment encoding the C terminus of the *GCN20* coding region tagged with the FLAG epitope by the technique of PCR fusion (53), using mutagenic oligonucleotides O105 and O106. The resulting *SnaBI*-*HindIII* fragment was inserted at the corresponding sites in the polylinker region of plasmid p2340, yielding plasmid Jp277. Both PCR-derived fragments in plasmids Jp259 and Jp277 were sequenced to confirm the presence of the desired mutations. Finally, the *SphI*-*BglII* fragment from plasmid Jp259, containing the G371D mutation, was inserted at the corresponding sites in Jp277, to yield p2343. Sequence analysis was carried out to confirm the presence of both G371D and G654D mutations in p2343.

Plasmids encoding protein fusions between the *Escherichia coli* *trpE* gene and *GCN1* were constructed by using the pATH vector system (28). The 2.7-kb *EcoRI* fragment from the 5' end of *GCN1* containing codons 170 to 1060 was subcloned from p1413 into the *EcoRI* site of pATH1, generating plasmid p1838. The 3.5-kb *BamHI*-*SalI* fragment from the 3' of *GCN1* containing codons 1617

TABLE 2. Yeast strains used

Strain	Genotype	Reference or source
F113 (TD28)	<i>MATa ino1 ura3-52 can1</i>	13
H1402	<i>MATα ino1 ura3-52 leu2-3 leu2-112</i>	21
H1511	<i>MATα ura3-52 trp1-Δ63 leu2-3 leu2-112</i>	19
H2079	<i>MATa ino1 ura3-52 can1 gcn1Δ</i>	31
H2512	<i>MATa ino1 ura3-52 can1 gcn20Δ</i>	47
ED800	<i>MATa ino1 ura3-52 can1 gcn20Δ trp1Δ::hisG</i>	This study
ED802	<i>MATa ino1 ura3-52 can1 gcn20Δ trp1Δ::hisG GCN4-lacZ::TRP1</i>	This study
ED1001	<i>MATa ino1 ura3-52 can1 gcn20Δ leu2Δ::hisG</i>	This study
HF7c	<i>MATa ura3-52 his3-200 ade2-101 lys2-801 trp1-901 leu2-3 leu2-112 gal4-542 gal80-538 LYS2::GAL1-HIS3 URA3::GAL4 17-mers₃-CYC1-lacZ</i>	16
TP11B-4-1	<i>MATa ade1 leu2-3 leu2-112 ura3-52 prt1-1</i>	G. Johnston; 19

to 2672 was subcloned from p1413 into *Bam*HI- and *Sal*I-digested pATH2, forming plasmid p1800.

Yeast strains. The strains used in this study are listed in Table 2. To construct ED802, the *TRP1* gene in H2512 was disrupted by transforming the strain to *Ura*⁺ *Trp*⁻ with plasmid pNKY1009 (1), and the transformants were grown on 5-fluoro-orotic acid medium (6) to obtain the *Ura*⁻ *Trp*⁻ derivative ED800. The *GCN4-lacZ* fusion on p1108 (11) was integrated at the *TRP1* locus by transforming ED800 to *Trp*⁺ with plasmid DNA digested with *Sna*BI to produce strain ED802. ED1001 was constructed from H2512 by using the *LEU2* disruption plasmid pNKY85 (1).

Isolation of *gcn1-G1444D*. Plasmid p2376 was used to transform the *E. coli* mutator strain XL1-Red (Stratagene), and DNA was isolated from approximately 47,500 pooled transformants. The *Xho*I-*Bst*XI fragment encoding part of the EF3-like region of *GCN1* was subcloned from the pooled mutagenized plasmids into unmutagenized p2376 digested with *Xho*I and *Bst*XI. Approximately 141,000 bacterial transformants were pooled, and plasmid DNA isolated from the pool was used to transform yeast strain H2079 to uracil prototrophy. Approximately 400 colonies were replica plated to medium containing 3-aminotriazole (3-AT); of these, 25 showed a 3-AT-sensitive (3-AT^s) phenotype. Plasmid p2395, containing the *gcn1-G1444D* allele, was isolated from one such mutant which could not grow on medium containing 30 mM 3-AT and grew poorly on medium containing 10 mM 3-AT.

Isolation of a human cDNA homologous to *GCN1*. Apparently identical IMAGE (integrated molecular analysis of genome expression) (30) clones 40567 and 41510 were obtained from the IMAGE Consortium (Lawrence Livermore National Laboratory). The sequence of the entire 1.7-kb cDNA in clone 40567 was obtained by using a Sequenase 2.0 kit (U.S. Biochemical). Primer MJM85, corresponding to the sequence of the noncoding strand 1.6 kb from the poly(A) tail, and adapter primer 1 (AP1) were used to PCR amplify human skeletal muscle cDNA by using a Marathon-Ready cDNA kit (Clontech). Touchdown PCR amplification (5 cycles at 72°C, 5 cycles at 70°C, and 25 cycles at 68°C) using an Advantage cDNA PCR kit and Advantage KlenTaq Polymerase (Clontech) resulted in a heterogeneous set of amplification products, which were purified through LMP-agarose (FMC) and cloned directly into plasmid pCRII, a TA-cloning vector (Invitrogen). Plasmid p2388 was found to contain a ca. 2.6-kb insert encoding a protein with extensive sequence similarity to *GCN1*. The sequence of the 5' end of the insert in p2388 was obtained and used to design primer MJM89, corresponding to the sequence of the noncoding strand at a position ≈4.0 kb from the poly(A) tail. MJM89 and primer AP1 were used in touchdown PCR as before, again yielding a heterogeneous set of amplification products which were purified and cloned into pCRII. Plasmid p2399, containing an approximately 2.1-kb insert, was isolated and the sequence of the insert was determined by Lofstrand Labs Limited.

Analysis of *GCN1* and *GCN20* regulatory function. Plasmid-borne *GCN1* or *GCN20* alleles were tested for complementation of *gcn1Δ* or *gcn20Δ* strains by replica-plating transformants to SD minimal medium containing 30 mM 3-AT and excess (40 mM) leucine as described previously (31). To measure expression of *GCN4-lacZ* fusions, β-galactosidase assays were conducted on whole-cell extracts prepared from exponentially growing cultures as previously described (31, 47).

Sucrose gradient analysis of yeast polysomes and ribosomes. Yeast cultures (300 ml) were grown in SD medium (plus supplements as required) at 28 to 30°C to an optical density at 600 nm (OD₆₀₀) of 1.0 ± 0.2. Typically, a saturated culture was diluted to an OD₆₀₀ of 0.04 and allowed to grow for 15 to 17 h with 225-rpm shaking. Five minutes before harvesting, cycloheximide was added to 83

μg per ml. Cultures were then transferred to 500-ml bottles, and ice chips were added to cool the culture and bring the final concentration of cycloheximide to 50 μg per ml. Cells were harvested by centrifugation at 5,000 rpm for 6 min at 4°C in a Sorvall GS3 rotor. The pellet was resuspended in 3 to 5 ml of growth medium, transferred to a 15-ml tube, and centrifuged at 4,000 rpm for 3 min at 4°C in a Jouan model CR412 centrifuge. Cells were washed once in 5 ml of breaking buffer (20 mM Tris-HCl [pH 7.5], 50 mM NaCl, 10 mM MgCl₂, 2 mM dithiothreitol, 0.5 mM phenylmethylsulfonyl fluoride, 1 μM pepstatin, 5 μM leupeptin, 0.15 μM aprotinin, 5 mM sodium molybdate, 5 mM sodium fluoride, 50 μg of cycloheximide per ml, 200 μg of heparin per ml) and centrifuged as before. After aspiration of the supernatant, 1 packed-cell volume of breaking buffer and 2 packed-cell volumes of glass beads were added (typically 600 μl of breaking buffer and 1.6 g of glass beads). Cells were vortexed by hand four times for 30 s each at 4°C, with incubation on ice water between each treatment. Unbroken cells were removed by centrifugation in microcentrifuge tubes at 1,000 rpm for 5 min in the Jouan centrifuge at 4°C. Fifteen OD₂₆₀ units of supernatant was layered on 12-ml linear 7 to 47% sucrose gradients prepared in breaking buffer lacking heparin and centrifuged in an SW41Ti rotor at 4°C at 39,000 rpm for 170 min. The gradients were scanned at 254 nm and separated into 600-μl fractions at a flow rate of 0.5 ml per ml with an Isco VA-5 gradient collector. For gradients including ATP, the nucleotide was added to the breaking buffer at 5 mM and to the gradients at 2.5 mM.

For experiments involving the *prt1-1* mutation, cultures were grown in SD medium plus supplements (0.3 mM adenine, 0.2 mM uracil, 0.5 mM isoleucine, 0.5 mM valine, and 2 mM leucine) at 23°C to an OD₆₀₀ of 1.0 and harvested by centrifugation in the Sorvall GS3 rotor at 5,000 rpm for 6 min at 20 to 22°C. Half of the resuspended cells was added to 150 ml of medium at 23°C, the other half was added to prewarmed 37°C medium, and both cultures were incubated for 30 min at the respective temperatures. Cycloheximide was added to 100 μg per ml 5 min before harvesting. Ice chips were added to cool the samples and bring the cycloheximide concentration to 50 μg per ml, and the remainder of the analysis was carried out as described above.

To analyze proteins in the gradient fractions, 50 μl of each was mixed with 4× loading buffer (250 mM Tris-HCl [pH 6.8], 6.25% sodium dodecyl sulfate [SDS], 40% glycerol, 1.4 M β-mercaptoethanol, 0.1% bromophenol blue), boiled for 2.5 min, and separated by polyacrylamide gel electrophoresis (PAGE) on 10% polyacrylamide gels (bisacrylamide/acrylamide, 1:118) containing SDS (31). The separated proteins were then subjected to immunoblot analysis as described below. In some cases, fractions were precipitated with trichloroacetic acid (TCA) prior to SDS-PAGE analysis as follows. Typically, 200 μl of each fraction was made 12.5% TCA by the addition of ice cold 100% solution. After 20 min on ice, samples were precipitated by centrifugation for 10 min at 14,000 × g in an Eppendorf Microfuge at 4°C. The supernatant was aspirated, and the tubes were respun to allow removal of residual amounts of TCA. Two microliters of unbuffered 1 M Tris base was added, and the samples were resuspended with vortexing in 20 μl of 2× urea buffer (50 mM Tris-HCl [pH 7.2], 1% SDS, 36% urea) prior to the addition of 20 μl of 2× loading buffer (125 mM Tris-HCl [pH 6.8], 4% SDS, 20% glycerol, 1.4 M β-mercaptoethanol, 0.1% bromophenol blue) and boiling for 2.5 min.

Antibodies. Anti-*GCN1* antisera HL1402 and HL1405, anti-*GCN20* antiserum HL1317, and anti-SUI2 antiserum were previously described (11, 47). Monoclonal antibodies against PUB2, a 60S ribosomal subunit protein (34), were a gift from Jim Anderson and have been described elsewhere (3). The anti-VAT2 monoclonal antibody 13D11 was generously supplied by Patty Kane (SUNY Health Science Center at Syracuse) and has been described previously (26). Antibodies against β-galactosidase were purchased from Promega.

To produce antibodies against the amino- and carboxy-terminal portions of *GCN1*, plasmids p1838 and p1800 were introduced into *E. coli* HB101 and *TrpE-GCN1* fusion proteins were induced and purified as described previously (28, 47). Five New Zealand White rabbits (HL1408, HL1409, and HL1410 for the C-terminal *GCN1* fusion; HL2171 and HL2172 for the N-terminal *GCN1* fusion) were injected with 1 mg of fusion protein and boosted at 4-week intervals by Hazelton Laboratories.

For immunofluorescence experiments, anti-*GCN1* antisera (HL1402 and HL1405) were preadsorbed with either fixed yeast cells or a boiled lysate prepared from the *gcn1Δ* strain H2079. The preadsorption to fixed cells was carried out as described previously (37) except that rabbit polyclonal serum was used. The preadsorbed antiserum was used directly or diluted 1:2 for immunofluorescence experiments (final dilution of sera was 1:100 to 1:200).

For immunoblotting and immunoprecipitation experiments, anti-*GCN1* serum was purified by using the Avid-AI matrix (UniSyn Technologies, Inc., Tustin, Calif.) according to the manufacturer's protocol. Briefly, 3 ml of crude rabbit antiserum was mixed with 1 ml of washed Avid-AI resin in phosphate-buffered saline (PBS) for 1 h at 23°C. The matrix was washed in 15 ml of PBS twice, and the bound immunoglobulin G (IgG) fraction was eluted with 1 ml of 50 mM sodium acetate (pH 2.8) for 10 min at 4°C with gentle mixing. The resin was removed by centrifugation, and to the supernatant were added 1/10 volume of unbuffered 1 M Tris base and purified bovine serum albumin (BSA; New England BioLabs) to 10 mg per ml.

Immunoblot analysis. Following SDS-PAGE, proteins were transferred to polyvinylidene difluoride membranes (Immobilion; Millipore) for 2.5 h in a MicroGenie transfer apparatus (Idea Scientific Co.) at 4°C in 1× transfer buffer (25

mM Tris, 192 mM glycine) containing 20% methanol. Membranes were routinely stained with Ponceau S (Sigma) to assess the efficiency of transfer. Proteins were detected by using rabbit polyclonal antiserum against GCN20 (HL1317 at 1:900), SUI2 (at 1:750), or GCN1 (Avid-AI-purified antisera HL1402 and HL1405, each at 1:1,000) or monoclonal antibody against PUB2 (at 1:5,000 dilution). Detection of antigen-antibody complexes was performed by using horseradish peroxidase-conjugated donkey anti-rabbit IgG antibodies (in the cases of GCN1, GCN20, and SUI2 antibodies) or sheep anti-mouse IgG antibody (for the PUB2 antibody) at a dilution of 1:5,000 (Amersham) with the ECL (enhanced chemiluminescence) system (Amersham) according to the vendor's protocols.

Indirect immunofluorescence. For localization of GCN1, yeast strain F113 and its isogenic *gcn1Δ* derivative H2079 were grown, fixed, harvested, converted to spheroplasts, permeabilized, and attached to polylysine-coated slides, all as described previously (37). Preadsorbed rabbit anti-GCN1 antiserum and mouse monoclonal anti-VAT2 antibody in PBS plus 0.5% BSA were incubated on the slides for 1 h. Cells were washed six times with PBS plus 0.5% BSA prior to the addition of a 1:200 dilution of fluorescein isothiocyanate-conjugated donkey anti-rabbit IgG and Texas red-conjugated donkey anti-mouse IgG for 1 h at room temperature in the dark. Cells were washed nine times with PBS plus 0.5% BSA, treated with 1 μg of 4',6'-diamidino-2-phenylindole (DAPI) per ml for 5 min, washed once, mounted with mounting medium, and sealed with clear nail polish. Microscopy was performed with a Zeiss Axiophot photomicroscope equipped with Nomarski optics and epifluorescence, using a 100× oil immersion lens. All fluorescent images were photographed for 40 to 60 s, using Eastman Kodak Co. (Rochester, N.Y.) Tri-X Pan ASA 400 film, increased to ASA 1600 by using Diafine developer.

Immunoprecipitations. Transformants of H2079 harboring different *GCN1* alleles were grown to early exponential phase and broken by vortexing with glass beads in TNM buffer (20 mM Tris-HCl [pH 7.5], 100 mM NaCl, 1 mM MgCl₂) supplemented with protease inhibitors as previously described (47). To immunoprecipitate c-Myc-tagged GCN1, protein samples (50 to 150 μg) were diluted to 0.75 ml in TNM buffer containing 0.25% Triton X-100 and 0.125% sodium deoxycholate and then precipitated with either 1 μg of mouse anti-Myc monoclonal antibody (clone 9E10; Oncogene Science) or a mixture of rabbit anti-GCN1 sera (3 μl each of HL1402, HL1405, and HL1410) which recognize different regions of the GCN1 protein for 1 to 2 h at 4°C with shaking. Immune complexes were collected after 1 h of incubation with either Protein-G Plus Agarose (Oncogene Sciences; for the c-Myc antibodies) or protein A-Sepharose (Pharmacia; for the rabbit polyclonal sera). The supernatant (representing the unprecipitated fraction) was TCA precipitated, washed twice with acetone, and dried. The pellet from the immunoprecipitation was washed twice with TNM buffer containing detergents and twice with TNM buffer alone. Samples were mixed with 2× loading buffer, boiled for 2 min, and fractionated on low-cross-linking SDS-10% polyacrylamide gels as described above.

Nucleotide sequence accession number. The complete nucleotide sequence determined in this study was deposited in GenBank with accession no. U77700.

RESULTS

Indirect immunofluorescence reveals cytoplasmic localization of GCN1. Because GCN20 is a member of the ABC family of proteins, we considered the possibility that the GCN1/GCN20 complex described previously (47) constitutes an ABC transporter that affects the cytosolic concentration of amino acids. According to this model, GCN20 would contribute the two ATP-binding domains, whereas the multiple hydrophobic segments present in GCN1 (31) would provide the MSDs of the transporter. To explore this possibility, we conducted indirect immunofluorescence on yeast cells with GCN1 antibodies to determine whether GCN1 is localized to a cellular membrane. Since we were particularly interested in the possibility that GCN1 and GCN20 comprise a vacuolar transporter, we localized VAT2 (VMA2), a known membrane-associated component of the vacuolar ATPase (52), in the same cells. The antibodies against GCN1 gave diffuse nonuniform cytoplasmic staining that did not appear to coincide with any cellular membrane and, in general, was excluded from both vacuoles (as visualized by Nomarski optics) and nuclei (as visualized by DAPI staining) (Fig. 1). These results were clearly distinguishable from the vacuolar membrane staining observed with antibodies against VAT2 (Fig. 1) and the endoplasmic reticulum staining seen with KAR2 antibodies (data not shown). The staining observed with GCN1 antibodies was specific, as no fluorescence was seen in cells of an isogenic *gcn1Δ* strain (Fig.

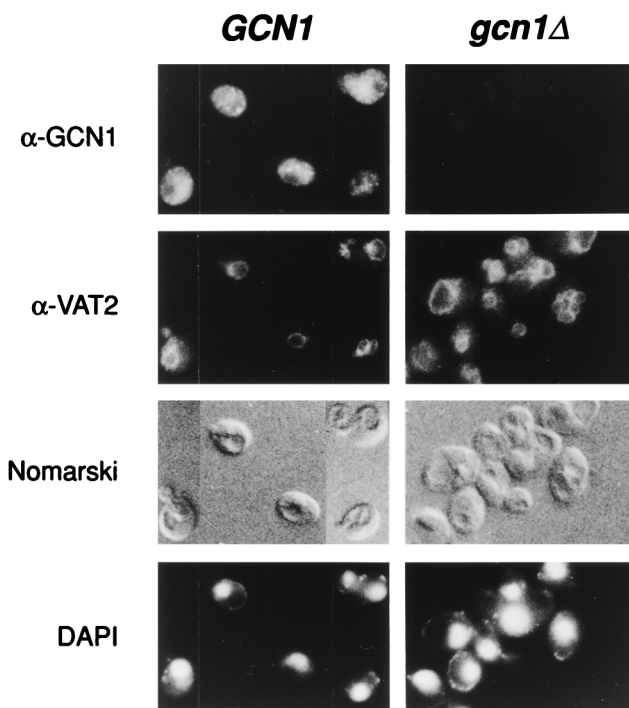


FIG. 1. Localization of GCN1 by indirect immunofluorescence microscopy of wild-type and *gcn1Δ* cells. Cells of wild-type strain F113 (left panels) and *gcn1Δ* strain H2079 (right panels) from cultures growing exponentially in YPD medium were fixed and stained with partially purified anti-GCN1 polyclonal serum H1405 (α -GCN1) and with anti-VAT2 monoclonal antibody 13D11 (α -VAT2) as described in Materials and Methods. Cells were photographed by using Nomarski optics, and nuclei were visualized by DAPI staining. GCN1 staining and VAT2 staining were observed by using fluorescein and rhodamine filter sets, respectively.

1). These results do not support a model in which GCN1 provides the MSDs of an ABC transporter.

The ABCs of GCN20 are largely dispensable for GCN20 regulatory function. In ABC transporters, the ABCs couple the energy of ATP hydrolysis to transport of molecules across a concentration gradient (23). We reasoned that if GCN20 provided the ABCs of an amino acid transporter, then deletion of these domains should eliminate the ability of the GCN1/GCN20 complex to stimulate *GCN4* expression in amino acid-starved cells. To test this idea, we constructed several truncations and internal deletions of *GCN20* on low-copy-number plasmids and tested their ability to complement a *gcn20Δ* strain for its inability to derepress *GCN4* and one of its target genes in the histidine biosynthetic pathway, *HIS3*. As seen in Fig. 2, deletions that removed one or both of the putative ABCs from GCN20 reduced but did not eliminate derepression of a *GCN4-lacZ* reporter in response to histidine starvation in medium containing 3-AT, an inhibitor of the *HIS3* product. In fact, the construct encoding only the N-terminal 118 residues of GCN20 (p1740) derepressed *GCN4-lacZ* expression to more than 50% of the wild-type level. These mutations only partially reduced the ability to derepress *HIS3*, as indicated by the level of 3-AT resistance. In contrast to these results, an internal deletion of N-terminal residues 4 to 118 completely abolished *GCN20* function as measured in both assays (Fig. 2, p2486). Immunoblot analysis of whole-cell extracts using GCN20 antibodies showed reduced expression of the mutant protein truncated at residue 596 (p1738) and that containing the Δ 4-118 deletion (p2486), whereas the proteins truncated at

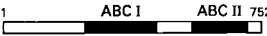


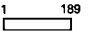
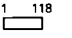

Construct	GCN20 Amino Acids Present	GCN20 Function			GCN20 Protein Expression	GCN20-lacZ Complexed with GCN1	
		3-AT ^r	GCN4-lacZ R	Expression DR % wt			
p1729 (wt)		+++	26	113	100	+++	+
p2485		+++	23	95	77	++	ND
p1738		+	21	60	33	+	ND
p1739		++	26	96	78	-*	+
p1740		+	23	77	54	-*	+
p2486		-	17	31	0	++	-
pRS316	Vector	-	17	34	0	-	NA

FIG. 2. Analysis of mutant GCN20 proteins for regulation of *GCN4* expression and interaction with GCN1. The *GCN20* deletion alleles are represented schematically by boxes depicting the encoded GCN20 proteins numbered from the amino terminus. Wild-type (wt) GCN20 is depicted at the top with its two ABCs shaded. Each allele was introduced on a low-copy-number plasmid into *gcn20Δ* strain ED802, and *GCN20* regulatory function was examined in two ways. Growth on SD medium containing 3-AT was measured by replica plating to SD medium containing 30 mM 3-AT and incubation for 2 to 3 days. The amount of growth (3-AT^r) was summarized as follows: + + +, wild-type growth; + +, good growth; +, modest growth; or -, little or no growth. β -Galactosidase activities were assayed in whole-cell extracts prepared from exponentially growing cells cultured on minimal medium, where *GCN4* is normally repressed (R), or on minimal medium containing 10 mM 3-AT, where *GCN4* is normally derepressed (DR). Enzyme activities are expressed as nanomoles of *o*-nitrophenyl- β -D-galactopyranoside hydrolyzed per milligram per minute. The values shown are the averages calculated from three independent transformants. The values indicated as % wt were calculated by (i) subtracting the *GCN4-lacZ* expression measured in the transformant containing vector alone from that measured for each construct under derepressing conditions and (ii) dividing these corrected values by the corrected value for the wild-type construct on p1729. GCN20 protein expression was determined by immunoblot analysis of whole-cell extracts using antibodies against GCN20. The results (data not shown) are summarized as follows: + + +, wild-type levels of GCN20 protein detected; + +, 50 to 80% of the level of wild-type GCN20 protein; +, 25 to 50% of the level of wild-type GCN20 protein; -, no GCN20 protein detected; -*, failure to detect GCN20. The results of coimmunoprecipitation experiments presented in Fig. 3 are summarized in the rightmost column. ND, not done; NA, not applicable.

positions 189 (p1739) and 118 (p1740) were undetectable (data not shown; results summarized in Fig. 2). The reduction in expression of the Δ 4-118 protein (p2486), however, cannot explain its complete loss of *GCN20* function because it was produced at the same level as was a full-length GCN20 protein containing Met and Arg substitutions at Ile-4 and Gly-5, respectively, that confers nearly wild-type *GCN20* function (p2485 [Fig. 2]). We attribute the failure to detect the GCN20 proteins truncated at residues 188 and 118 to loss of epitopes recognized by our GCN20 polyclonal antibodies, which were raised against GCN20 residues 1 to 457, to two reasons: (i) both constructs exhibit >50% of wild-type *GCN20* function, and (ii) the construct truncated at position 118 conferred wild-type 3-AT resistance when introduced on a high-copy-number plasmid (data not shown). We conclude that the interval from positions 4 to 118 in GCN20 contains residues critical for its regulatory function, whereas the remainder of the protein containing the two ABCs is largely dispensable for GCN20-mediated derepression of *GCN4* expression in histidine-starved cells. This conclusion is in accordance with the fact that *gcn20-1*, the only characterized *Gcn*⁻ allele isolated in vivo, bears a frameshift mutation that truncates the coding sequence after residue 96. Given that the ABCs in GCN20 are dispensable for its regulatory function in histidine-starved cells, it seems unlikely that the GCN1/GCN20 complex functions as a membrane transporter in regulating *GCN4* translation.

Our finding that the N-terminal 118 amino acids of GCN20 are sufficient for its regulatory function implied that this small segment of GCN20 should be sufficient for complex formation with GCN1. Supporting this prediction, we showed previously that the N-terminal 118 residues of GCN20 are sufficient for an interaction with the C-terminal two-thirds of GCN1 in the yeast two-hybrid system (47). We wished to verify this conclusion by using a different assay and also to determine whether the N-terminal segment of GCN20 is both necessary and sufficient for complex formation with GCN1. Accordingly, we investigated whether β -galactosidase fusion proteins contain-

ing different N-terminal segments of GCN20 could be coimmunoprecipitated with GCN1 from whole-cell extracts. As shown in Fig. 3, the N-terminal 96 residues in GCN20 were sufficient for immunoprecipitation of the GCN20(1-96)-LacZ fusion protein, using antibodies against GCN1. By comparing the efficiencies of coimmunoprecipitation for the different fusions, we found that truncating GCN20 from position 457 to

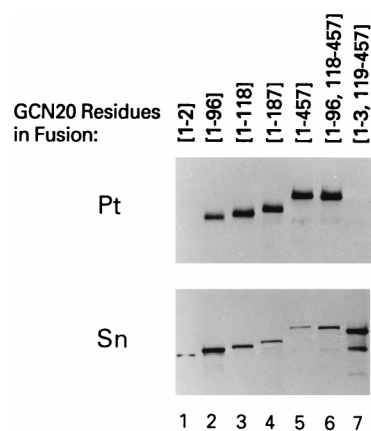


FIG. 3. The N-terminal segment of GCN20 is necessary and sufficient for complex formation with GCN1. *GCN20-lacZ* constructs encoding the indicated segments of GCN20 (with amino acids numbered from the N terminus) fused to β -galactosidase were introduced into *gcn20Δ* strain H2512. Whole-cell extracts were prepared from exponentially growing cells of each transformant cultured in SD medium with minimal supplements, and 20 μ g of total protein was immunoprecipitated by using anti-GCN1 antibodies and protein A-Sepharose beads. Proteins remaining in the supernatant were precipitated by the addition of TCA to 5%. Samples were resolved by SDS-PAGE (8% gel), transferred to nitrocellulose, and probed with anti- β -galactosidase antibodies. Immune complexes were visualized by enhanced chemiluminescence. Pt, pellet; Sn, supernatant. The constructs encoding GCN20-LacZ fusion proteins analyzed were p1922 (lane 1), p2488 (lane 2), p2487 (lane 3), Jp233 (lane 4), p1924 (lane 5), p2491 (lane 6), and Jp237 (lane 7).

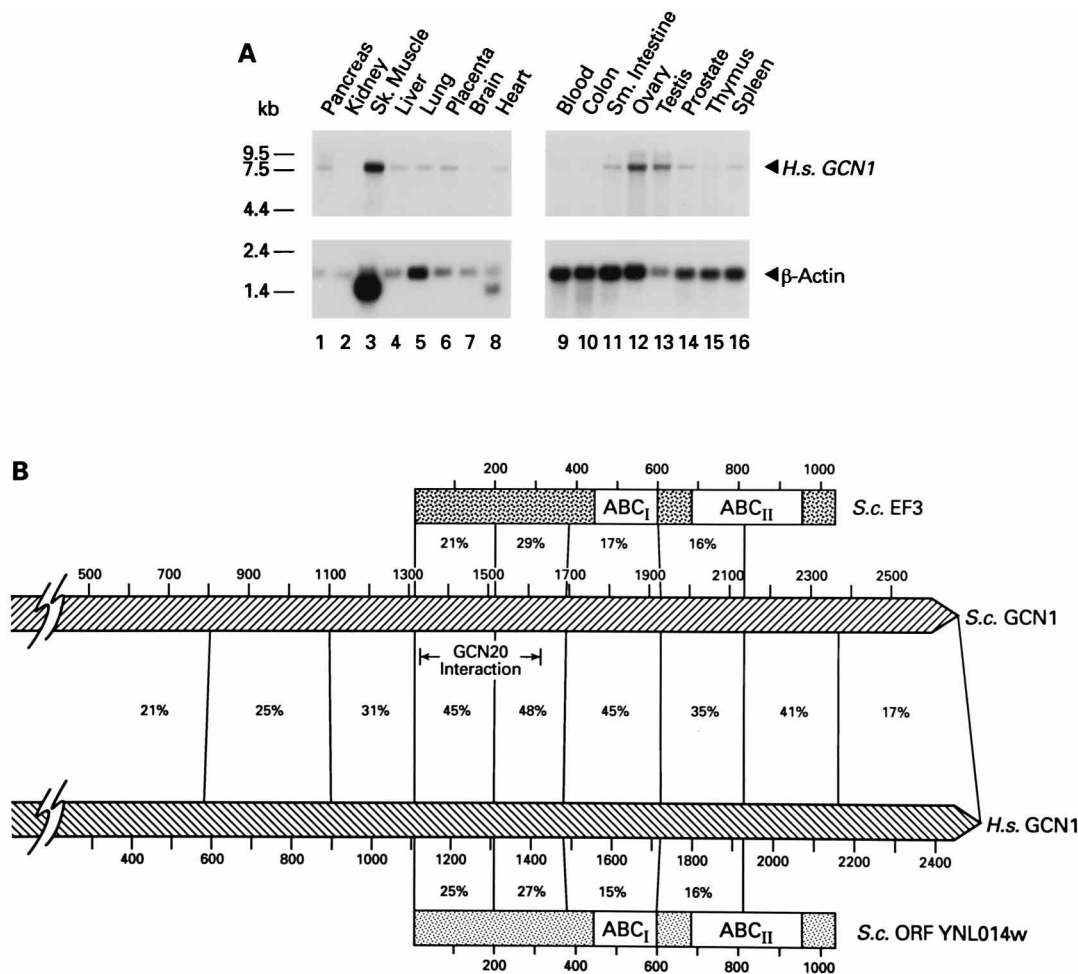


FIG. 4. Characterization of a human GCN1 homolog. (A) Northern blot analysis of poly(A)⁺ RNA from human tissues probed with a portion of the *H.s. GCN1* cDNA. A Multiple Tissue Northern blot (Clontech) containing 2 μ g of poly(A)⁺ RNA isolated from each of the indicated tissues was probed with radiolabeled 0.6-kb *Bam*HI-*Hind*III fragment of IMAGE clone 40567, containing the sequences 1.0 to 1.6 kb 5' to the poly(A) tail of the *H.s. GCN1* cDNA, or with a 2-kb fragment of the human β -actin gene, according to the vendor's instructions. The positions of molecular weight markers are shown on the left. Sk., skeletal; Sm., small. (B) Summary of sequence similarities between *H.s. GCN1* and *Saccharomyces GCN1* and EF3 sequences. The rectangular boxes represent the complete sequences of *S. cerevisiae* EF3 (S.c. EF3) and ORF YNL014w, the C-terminal 85% of *S. cerevisiae* GCN1 (S.c. GCN1), and *H.s. GCN1*. The percentage sequence identities shown between pairs of sequences in different intervals were calculated by using the BESTFIT program (12). The DNA sequence determined for *H.s. GCN1* (GenBank accession no. U77700) is 99.8% identical (over the region that we sequenced) to that determined by Nomura et al. (GenBank accession no. D86973). The latter deduced amino acid sequence differs from ours in containing 582 additional codons at the N terminus, 5 missense changes, and a frameshift at the C terminus. The composite *H.s. GCN1* sequence used to construct the alignments depicted here was obtained by appending the first 582 codons from the sequence of Nomura et al. to the N terminus of the 1,928 codons we determined, giving a total sequence length of 2,510 codons.

either 187, 118, or 96 led to a progressive decrease in the yield of the GCN1/GCN20-LacZ complex (Fig. 3; compare lanes 2 to 5). This finding suggests that residues C terminal to position 96 may contribute to the stability of the GCN1-GCN20 interaction. Removing residues 4 to 118 completely abolished immunoprecipitation of the GCN20(1-457)-LacZ fusion protein with GCN1 antibodies (Fig. 3, lane 7), indicating that this N-terminal segment of GCN20 is necessary, as well as sufficient, for complex formation with GCN1. Taken together, the results in Fig. 2 and 3 indicate that the only portion of GCN20 crucial for regulatory function is the N-terminal segment that anchors the protein to GCN1. As discussed below, the ABC domains in GCN20 may serve to modulate GCN1 function by controlling the extent or duration of GCN2 activation in amino acid-starved cells, or they may mediate a response to signals other than amino acid starvation.

The EF3-like domain is conserved in a human homolog of GCN1. The *GCN1* gene encodes a 297-kDa protein containing

a segment of more than 800 amino acids with significant sequence similarity to EF3. The regions of highest similarity between the two proteins involve the N-terminal one-third of EF3 and the segment of GCN1 between residues 1330 and 1641, over which the two proteins are 26% identical (31). Henceforth, we refer to this segment as the EF3-like region of GCN1. In support of the idea that the similarity to EF3 is relevant to *GCN1* regulatory function, we isolated a human cDNA encoding a protein highly related to GCN1 that also contains an EF3-like region. Two clones containing the 3' end of this cDNA were identified by searching a database of expressed sequence tags (dbEST) (7) for GCN1-related sequences, using the BLAST program (2). We probed a Northern blot containing poly(A)⁺ RNA isolated from different human tissues with a radiolabeled restriction fragment from one of the clones; as shown in Fig. 4A, the cDNA probe hybridized to a ca. 8.0-kb transcript in a variety of tissues, similar in length to *Saccharomyces GCN1* mRNA (\approx 8.5 kb

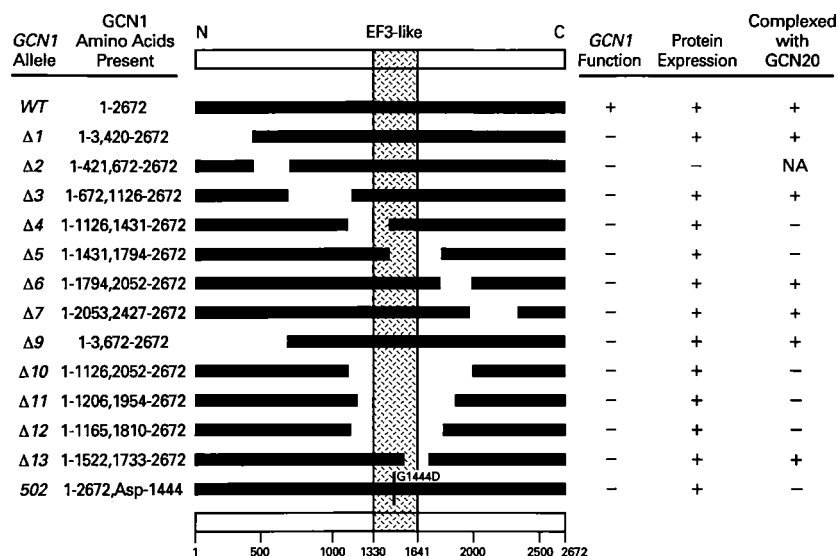


FIG. 5. Analysis of internally deleted GCN1 proteins for in vivo regulatory function and complex formation with GCN20. The open rectangular boxes at the top and bottom represent the GCN1 protein from its amino (N) to carboxy (C) terminus, with the amino acid residues numbered across the bottom. The region of GCN1 with greatest similarity to EF3, corresponding to residues 1330 to 1641 (31), is indicated by the vertical hatched box. The solid rectangles represent the GCN1 residues present in the wild-type (WT) and retained in the various deletion derivatives of GCN1 (designated on the left as $\Delta 1$ to $\Delta 13$). The *gcn1-502* allele encodes a full-length GCN1 protein with Asp substituting for Gly-1444. Each GCN1 allele was introduced on a low-copy-number plasmid into *gcn1* Δ strain H2079, and the resulting transformants were replica plated to SD medium containing 30 mM 3-AT. The results shown under "GCN1 Function" indicated that all of the *gcn1* mutant alleles were indistinguishable from vector alone, failing to confer any detectable 3-AT resistance on H2079. Whole-cell extracts from the same transformants were analyzed for GCN1 protein expression by immunoblot analysis, and the results presented in Fig. 6 are summarized here under "Protein Expression" as + (wild-type or near wild-type levels of GCN1 detected) or - (no or little GCN1 detected). The ability of GCN20 to coimmunoprecipitate with the mutant or wild-type GCN1 proteins from cell extracts was examined by using anti-GCN1 antibodies, and the results presented in Fig. 7 are summarized here under "Complexed with GCN20" as + (GCN20 found in the immunoprecipitate), - (essentially no GCN20 found in immunoprecipitate under identical conditions), or NA (not applicable).

[31]). We used PCR amplification to isolate two additional overlapping clones from a pool of human skeletal muscle cDNAs (see Materials and Methods for details); the sequence assembled from all three clones encodes an ORF of 1,928 codons that is 35% identical to GCN1 over nearly its entire length. A cDNA sequence nearly identical to the one that we determined, but longer at the 5' end, was deposited in GenBank by N. Nomura and colleagues of the Kazusa DNA Research Institute, Chiba, Japan (accession no. D86973). We combined the two predicted amino acid sequences and aligned the resulting composite sequence of 2,510 codons (henceforth referred to as *H.s.GCN1*) with GCN1, EF3, and the closest relative of EF3, encoded by ORF YNL014w (Fig. 4B). The region of highest similarity between GCN1 and its human homolog encompasses the region of greatest similarity between GCN1 and EF3. Moreover, *H.s.GCN1* itself shows significant similarity to EF3 and YNL014w (Fig. 4B). Like GCN1, *H.s.GCN1* does not contain the conserved Walker motifs in the ABCs that are critical for nucleotide binding and hydrolysis (18) and is most similar to the portion of EF3 located N terminal to the ABC domains. The fact that an EF3-like segment is the region most highly conserved between GCN1 and its human homolog suggests that some aspect of GCN1 function is related to the activity of EF3 in translation elongation.

The EF3-like region of GCN1 is necessary and sufficient for interaction with GCN20. Considering that the ABCs in GCN20 are very similar to those in EF3, we wished to determine whether the N-terminal domain of GCN20 might interact with the EF-3 like region of GCN1. To address this possibility, we constructed a c-Myc epitope-tagged version of GCN1 on a low-copy-number plasmid and produced a series of internal deletions in the coding sequences of this tagged allele. We verified that the full-length c-Myc-tagged allele was indistin-

guishable from wild-type GCN1 in complementing the 3-AT sensitivity of a *gcn1* Δ strain (data not shown). As shown in Fig. 5, none of the deletion alleles could complement a chromosomal *gcn1* Δ allele and restore growth on medium containing 3-AT. Immunoblot analysis of whole cell extracts showed that all but one allele (*gcn1*- $\Delta 2$) produced GCN1 proteins at levels similar to that of chromosomally encoded wild-type GCN1 (Fig. 6). (The *gcn1*- $\Delta 2$ product was undetectable [data not shown].) Previously, we found that a GCN1 allele truncated after residue 2400, and thus missing the C-terminal 10% of the protein, was partially functional (31a). Therefore, in contrast to our findings for GCN20 (Fig. 2), at least 90% of the GCN1 protein is required for its regulatory function.

GCN1 proteins with internal deletions were then tested for the ability to form a stable complex with GCN20 by immunoprecipitating cell extracts with antibodies against GCN1 and probing the immune complexes with antibodies against GCN20. As shown in Fig. 7A, GCN20 was coimmunoprecipitated with only six of the internally deleted GCN1 proteins ($\Delta 1$, $\Delta 3$, $\Delta 6$, $\Delta 7$, $\Delta 9$, and $\Delta 13$). The same conclusion was reached from experiments using c-Myc antibodies to immunoprecipitate the GCN1 proteins (data not shown). In accordance with these findings, the five strains bearing GCN1 derivatives incapable of complex formation with GCN20 showed lower steady-state levels of GCN20 protein than did those containing mutant GCN1 proteins capable of interacting with GCN20 (Fig. 6). We showed previously that GCN20 is less stable in extracts of *gcn1* Δ strains, presumably due to increased proteolysis of non-complexed GCN20 (47). Inspection of the regions deleted in the mutant proteins that failed to complex with GCN20 ($\Delta 4$, $\Delta 5$, $\Delta 10$, $\Delta 11$, and $\Delta 12$) strongly suggested that the region encompassing the EF3-like domain in GCN1 is necessary for its ability to interact with GCN20 (summarized in Fig. 5). The

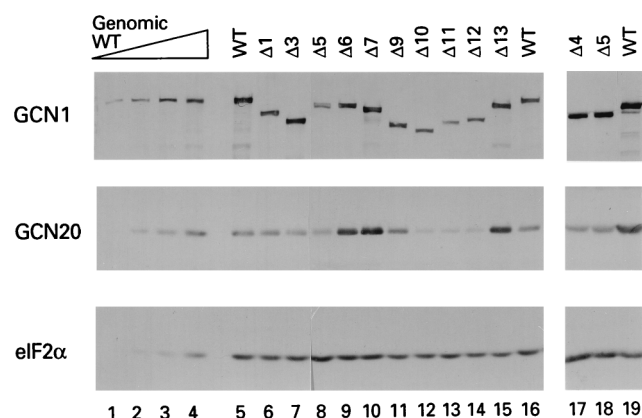


FIG. 6. Immunoblot analysis of GCN1 and GCN20 protein levels in cells expressing various *GCN1* deletion alleles. Transformants of *gcn1Δ* strain H2079 containing the indicated *GCN1* alleles on low-copy-number plasmids were grown to mid-logarithmic phase in SD medium containing minimal supplements, and whole-cell extracts were prepared. Fifty micrograms of total proteins was separated by SDS-PAGE (10% gel) followed by immunoblot analysis using antibodies against GCN1, GCN20, or eIF2 α , as indicated at the left. Immune complexes were visualized by enhanced chemiluminescence (Amersham). Lanes 1 to 4 contain 6.25, 12.5, 25, and 50 μ g, respectively, of total protein from strain F113 (the isogenic parent of strain H2079 containing *GCN1* at its normal chromosomal locus) that was analyzed in parallel (Genomic WT). The plasmid-borne wild-type (WT) *GCN1* allele expresses GCN1 at a level severalfold higher than that expressed from chromosomal *GCN1* in F113 (lane 5 versus lane 4). In an effort to ensure equal recognition of the internally deleted GCN1 proteins by the GCN1 antibodies, we used a mixture of three GCN1 antisera recognizing the N terminus (serum HL2171), C terminus (serum HL1410), or central domain of GCN1 containing the EF3-like region (serum HL1402).

fact that the *gcn1-Δ13* protein interacts with GCN20 suggests that residues C-terminal to position 1522 in the EF3-like region of GCN1 are dispensable for complex formation, at least in the presence of all residues N terminal to this site. It is interesting that deletions of residues C terminal to the EF3-like domain ($\Delta 6$, $\Delta 7$, and $\Delta 13$) led to higher than wild-type levels of GCN20 protein (Fig. 6). Perhaps these deletions alter the GCN1/GCN20 complex in a way that protects GCN20 from proteolysis.

In an effort to identify specific amino acids in the EF3-like domain of GCN1 critically required for the interaction with GCN20, plasmid p2367 containing the c-Myc epitope-tagged allele of *GCN1* was subjected to random mutagenesis using an *E. coli* mutator strain, and restriction fragments encompassing the EF3-like region were subcloned into unmutagenized p2367 to isolate mutations localized to this region of *GCN1*. The resulting pool of mutagenized plasmids was screened in *gcn1Δ* strain H2079 for the 3-AT^s phenotype, indicating failure to derepress *GCN4* expression. Plasmids rescued from two 3-AT^s transformants thus identified were shown to confer a 3-AT^s phenotype when reintroduced into H2079, confirming the presence of plasmid-borne *gcn1* alleles. Whole-cell extracts prepared from these mutants were immunoprecipitated with GCN1 antibodies to determine whether the mutant GCN1 proteins were capable of complex formation with GCN20. The results in Fig. 7B indicated that the mutant protein encoded by *gcn1-501* showed reduced interaction, whereas the *gcn1-502* product was almost completely defective for complex formation with GCN20. In addition, the steady-state level of GCN20 was greatly reduced in the *gcn1-502* extract, typical of *gcn1* null mutants (data not shown). DNA sequence analysis of the *gcn1-502* allele revealed a single mutation that replaces Gly-1444 with Asp in the EF3-like domain; henceforth, we refer to this allele as *gcn1-G1444D*. Gly-1444 is at a con-

served position in the region of highest sequence similarity between GCN1 and EF3 (Fig. 4B). We did not analyze *gcn1-501* further.

We next used the yeast two-hybrid method to determine whether the EF3-like region of GCN1 is sufficient for interaction with GCN20. We showed previously that a large fragment of GCN1 containing residues 672 to 2672 fused to the GAL4 DNA-binding domain interacted with the N-terminal 118 residues of GCN20 fused to the GAL4 activation domain by the two-hybrid assay (47). As shown in Fig. 8, two much smaller segments containing only the EF3-related domain of GCN1 (residues 1330 to 1669 and 1330 to 1617) showed equally strong interactions with the N-terminal 118 residues of GCN20. Combining these findings with results of the coimmunoprecipitation analysis summarized in Fig. 5, we conclude that the EF3-like region of GCN1 is both necessary and sufficient for complex formation with the N-terminal 118 residues of GCN20. This finding directly establishes the functional importance of this segment of GCN1.

Ribosome association of GCN1 and GCN20. Given that GCN1 and GCN20 are both related to EF3, and that GCN20 binds to the EF3-related segment of GCN1, we considered the possibility that GCN1 and GCN20 function on the ribosome in regulating GCN2 kinase activity. To investigate this possibility, we asked whether any of the GCN1 and GCN20 present in whole-cell extracts cosediment with polysomes fractionated by velocity sedimentation on sucrose gradients. The amounts of GCN1, GCN20, and the 60S ribosomal subunit protein PUB2 (34) in fractions collected from these gradients were analyzed by immunoblot analysis with antibodies against these proteins. As shown in Fig. 9A, most of the GCN1 and GCN20 sedimented more slowly than free 40S and 60S ribosomal subunits in fractions 3 to 6; however, a proportion of each protein was also found in fractions 11 to 19 containing 80S ribosomes and polysomes. The distributions of GCN1 and GCN20 differed in

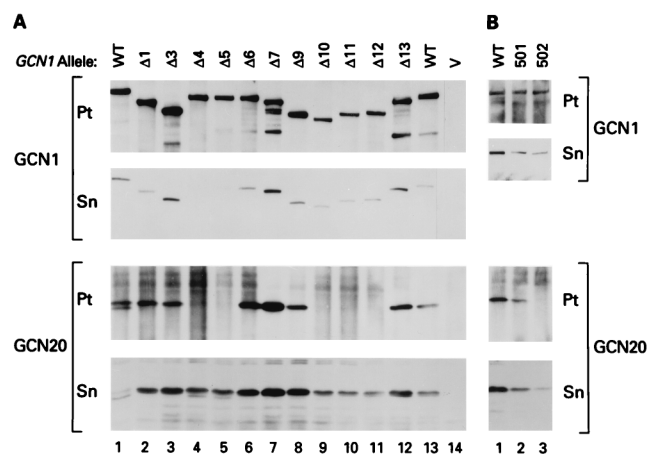


FIG. 7. Coimmunoprecipitation of GCN20 with mutated GCN1 proteins. (A) Whole-cell extracts were prepared from transformants of the *gcn1Δ* strain H2079 containing the plasmid-borne *GCN1* alleles depicted in Fig. 5. One hundred micrograms of total protein was immunoprecipitated with the mixture of three different GCN1 antisera described in the legend to Fig. 6. Proteins in the supernatant were precipitated by the addition of TCA to 12.5%. Samples were separated by SDS-PAGE (10% gel), transferred to Immobilon membranes, and probed with polyclonal antisera against GCN1 (top panels) or GCN20 (bottom panels). Immune complexes were visualized by enhanced chemiluminescence (Amersham). WT, wild type; V, vector alone; Pt, pellet; Sn, supernatant. (B) Exactly as in panel A except that the *GCN1* mutant alleles contain point mutations (Asp-1444 in the case of *gcn1-502* and uncharacterized for *gcn1-501*) rather than deletions, and aliquots of cell extracts containing 150 μ g of total protein were used in the immunoprecipitations.

Construct	GCN1 Segments Fused to GAL4-DBD	Two-hybrid Interaction			
		3-AT ^r		β-galactosidase Activity (U)	
		pACT-GCN20	pACT	pACT-GCN20	pACT
p1809	672 EF3-like 2672	+	-	34	0.63
p1816	672 2057	+	-	5.9	0.03
p1817	1330 1669	+	-	63	0.73
p2369	1330 1617	+	-	ND	

FIG. 8. The EF3-like region of GCN1 is sufficient for interaction with GCN20 in the yeast two-hybrid system. Strain HF7c containing *HIS3* and *lacZ* reporter genes bearing GAL4 DNA-binding sites was transformed with plasmids encoding the GAL4 DNA-binding domain fused to the portions of GCN1 depicted schematically together with plasmid pACTII encoding the GAL4 activation domain alone (pACT) or with plasmid p1825 encoding the first 118 residues of GCN20 fused to the GAL4 activation domain (pACT-GCN20). The GCN1 segments present in the GAL4 DNA-binding domain constructs are identified by the amino acid residues (numbered from the N terminus) present in each fusion. Two-hybrid interactions were detected by assaying transformants for growth on medium containing 3-AT and by measuring β-galactosidase activity in whole-cell extracts. +, growth on medium containing 30 mM 3-AT; -, little or no growth under the same conditions. For β-galactosidase assays, cells were grown exponentially in SD medium supplemented with adenine at 0.1 mM prior to the preparation of extracts. The mean values obtained from three independent transformants are reported. Units of β-galactosidase activity are expressed as nanomoles of *o*-nitrophenyl-β-D-galactopyranoside hydrolyzed per milligram of protein per minute. To provide a negative control for interactions with GCN20, plasmid pSE1112 (encoding a GAL4-SNF1 fusion) was analyzed in parallel. This construct gave 0.02 U of β-galactosidase activity in combination with pACT-GCN20 (p1825) and 0.08 units in combination with pACTII.

that a greater proportion of GCN1 was present in the fractions containing monosomes and disomes than in those containing the larger polysomes; in addition, a proportion of GCN1 was present in the fractions containing 60S subunits. To obtain evidence that GCN1 and GCN20 are associated with polysomes and not with some other rapidly sedimenting species, we treated the extracts with RNase A before centrifugation to digest the polysomes to 80S ribosomes. RNase digestion elim-

inated the polysomes, except for a small fraction of disomes, and led to a large accumulation of 80S ribosomes (Fig. 9B). Likewise, RNase digestion removed all of the GCN1 and GCN20 from fractions 15 to 19 and led to accumulation at the positions of 80S ribosomes and 60S subunits in the case of GCN1 and at the positions of 80S ribosomes and disomes in the case of GCN20 (Fig. 9B). The fact that GCN1 and GCN20 do not show identical distributions throughout the monosomal

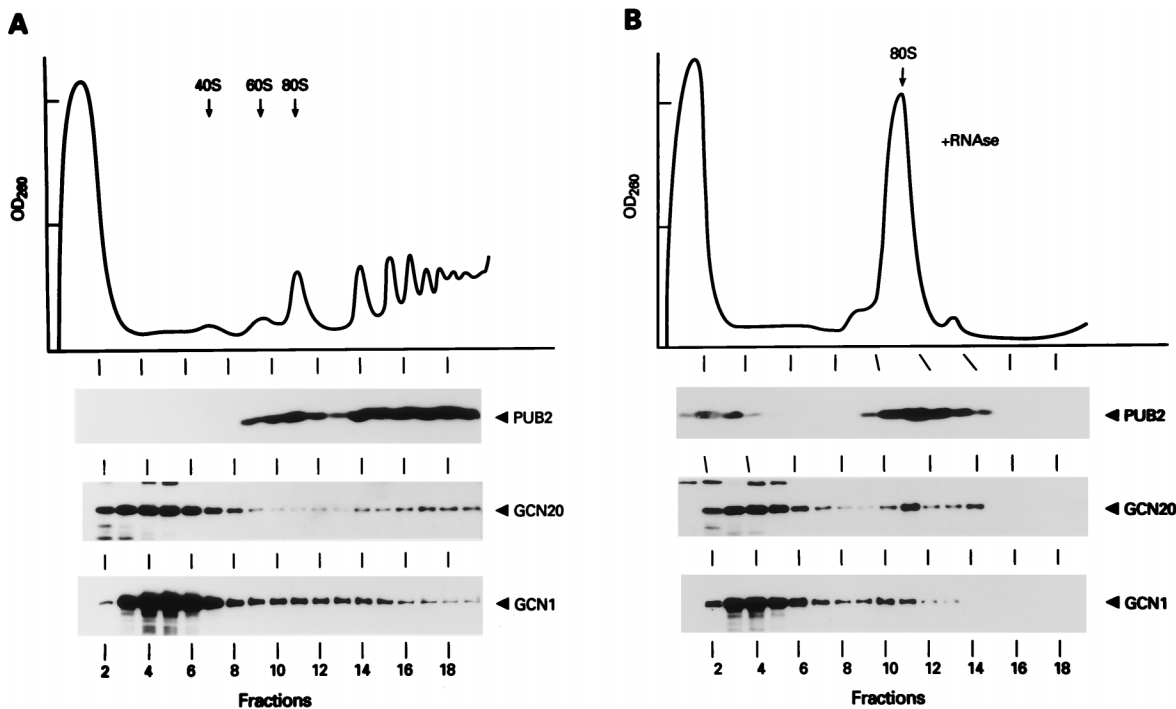


FIG. 9. Cosedimentation of GCN1 and GCN20 with ribosomes. (A) Whole-cell extracts were prepared from wild-type strain F113 and subjected to velocity sedimentation through preformed sucrose density gradients. Gradients were fractionated while scanning at 254 nm, and the resulting absorbance profiles are shown, with the top of the gradients on the left and the fraction numbers indicated across the bottom. Positions of 40S, 60S, and 80S ribosomal species are indicated by arrows. Fifty microliters of each fraction was analyzed by SDS-PAGE and immunoblotting using monoclonal antibodies against PUB2 (a 60S ribosomal subunit) or polyclonal antibodies against GCN1 or GCN20, as indicated on the right. Immune complexes were detected by enhanced chemiluminescence (Amersham). (B) The analysis was carried out exactly as for panel A except that the extract was incubated with RNase A at 125 μg of RNase A per 15 OD₂₆₀ units of extract for 15 min at 4°C prior to centrifugation.

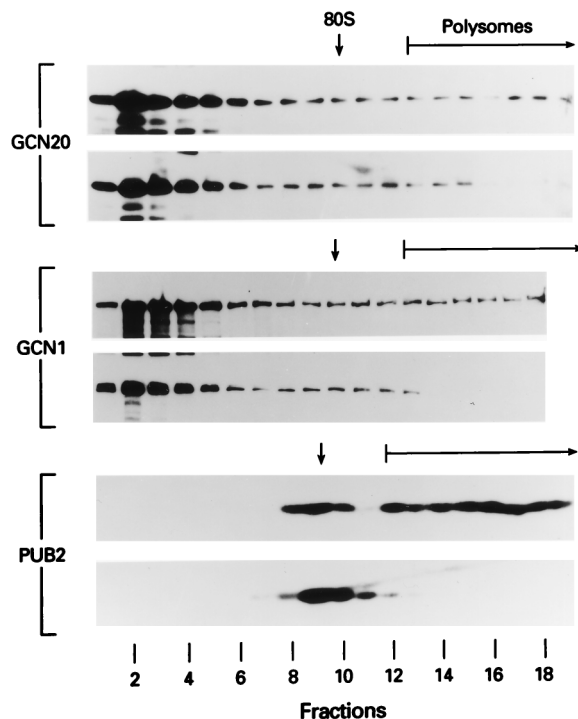


FIG. 10. A temperature-sensitive mutation that abolishes polysomes in vivo eliminates the fractions of GCN1 and GCN20 that cosediment with polysomes. The *prt1-1* strain TP11B-4-1 was grown at the permissive temperature (23°C) to an OD_{600} of ~1.0, after which half of the culture was shifted to the nonpermissive temperature (37°C) for 30 min and half continued at the permissive temperature, as described in Materials and Methods. Whole-cell extracts were prepared and fractionated by velocity sedimentation through sucrose gradients, and 50 μ l of each fraction was analyzed for GCN1, GCN20, and PUB2 proteins (as indicated to the right) by SDS-PAGE and immunoblot analysis using the appropriate antibodies, as described for Fig. 9. The positions of 80S ribosomes and polysomes in the gradients determined from the UV absorbance profiles (data not shown) are indicated. The numbers across the bottom indicate the gradient fractions from top to bottom.

and polysomal fractions in these experiments will be addressed below.

To provide additional evidence that GCN1 and GCN20 interact with polysomes, we eliminated polysomes in vivo by incubating a mutant strain with a temperature-sensitive mutation in the *PRT1*-encoded subunit of translation initiation factor eIF3 (32) at the restrictive temperature prior to harvesting the cells. Incubation of the *prt1-1* mutant at 37°C led to loss of large polysomes and accumulation of 80S ribosomes (Fig. 10, PUB2 panels), due to the fact that translation initiation, but not elongation, is impaired by the *prt1-1* mutation (17). In accordance with the idea that GCN1 and GCN20 interact with polysomes, we found that both proteins were eliminated from fractions at the bottom of the gradient in parallel with the loss of polysomes in the *prt1-1* mutant at 37°C (Fig. 10). It is noteworthy that GCN1 and GCN20 did not accumulate at the position of 80S ribosomes in the *prt1-1* extracts, in contrast to what occurred when polysomes were dissociated to 80S ribosomes by RNase treatment (Fig. 9B). These results may indicate that GCN1 and GCN20 have greater affinity for translating 80S ribosomes bound to mRNA than for nontranslating 80S couples lacking mRNA which accumulate when translation initiation is inhibited by the *prt1-1* mutation (19).

Because GCN20 contains putative ABCs, we asked whether

the ribosome association of GCN1 and GCN20 could be enhanced by addition of ATP to the sucrose gradients during centrifugation. As shown in Fig. 11, the addition of ATP greatly stimulated the proportions of GCN1 and GCN20 that cosedimented with polysomes, such that the majority of both proteins were now present in the polysomal fractions. Treatment of the extracts with RNase A confirmed that the increased amounts of rapidly sedimenting GCN1 and GCN20 seen in the presence of ATP were polysome associated (Fig. 11, +ATP +RNase panels). Neither ADP nor a nonhydrolyzable analog of ATP (5-adenylylimidodiphosphate [AMP-PNP]) conferred any stimulation of ribosome binding by GCN1 or GCN20 (data not shown). The polysome association of GCN20 was largely dependent on the presence of GCN1, since only a small fraction of GCN20 was present in the polysomal fractions in extracts prepared from a *gcn1 Δ* strain, whether or not ATP was added to the gradients (Fig. 12A and data not shown). The *gcn1-G1444D* mutation, which reduced the ability of GCN20 to complex with GCN1 (Fig. 7B), also

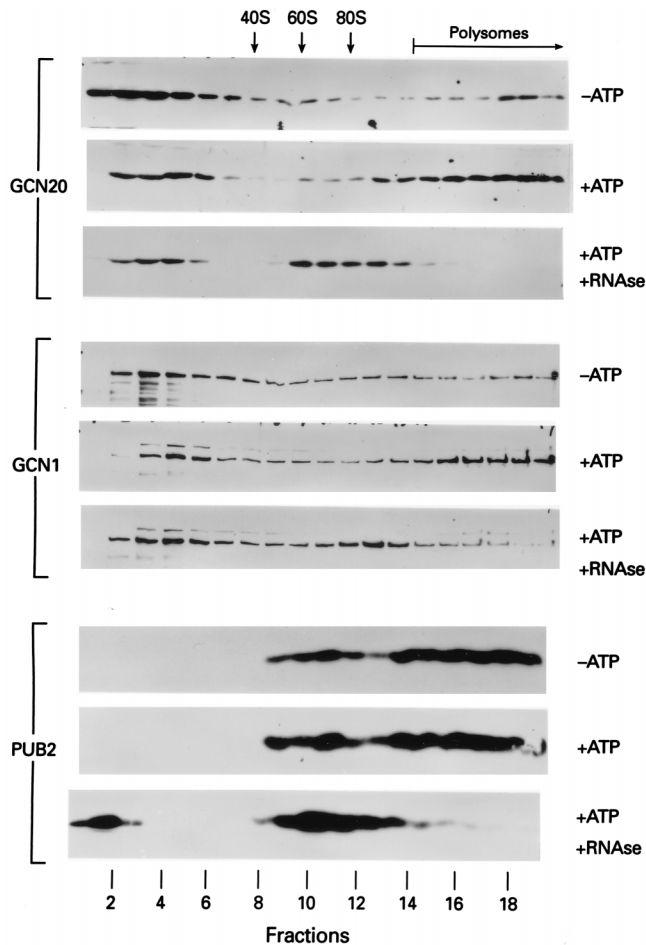


FIG. 11. The ribosome association of GCN1 and GCN20 is stimulated by ATP. Whole-cell extracts were prepared from wild-type strain F113, treated with RNase A where indicated, and fractionated by velocity sedimentation in sucrose density gradients as described for Fig. 9 except that ATP was included in the cell breaking buffer at 5 mM and in the sucrose gradients at 2.5 mM. Arrows indicate the positions of 40S and 60S subunits, 80S ribosomes, and polysomes, as determined from the UV absorbance profiles of the gradients (data not shown). Fifty microliters of each fraction was analyzed by SDS-PAGE and immunoblotting using antibodies against GCN1, GCN20, or PUB2 (indicated at the left) as described in the legend to Fig. 9. The numbers across the bottom indicate the gradient fractions from top to bottom.

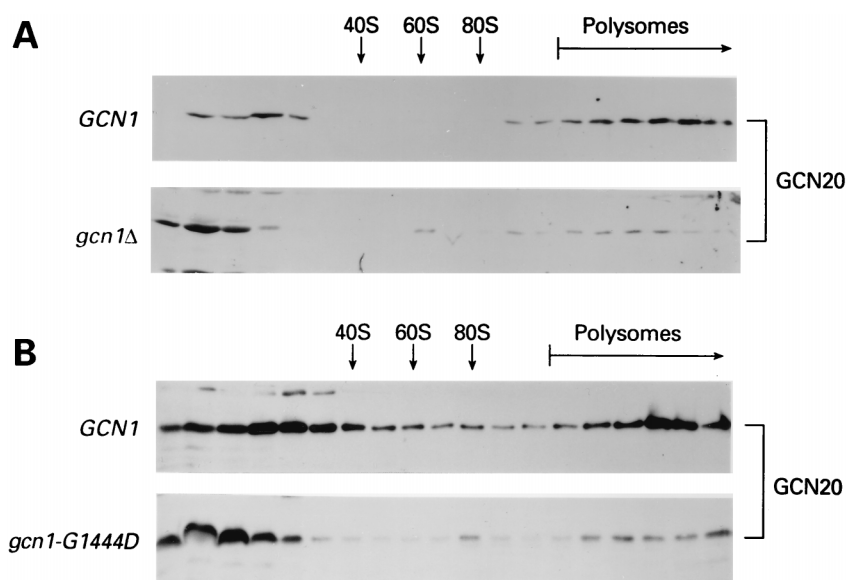


FIG. 12. Polysome association of GCN20 is reduced by *gcn1* mutations. (A) Effect of a *gcn1*Δ deletion. Whole cell extracts from strains F113 (*GCN1*) and H2079 (*gcn1*Δ) were prepared and fractionated by velocity sedimentation in sucrose density gradients in the presence of ATP, as described for Fig. 11. Arrows indicate the positions of 40S and 60S subunits, 80S ribosomes, and polysomes, as determined from the UV absorbance profiles of the gradients (data not shown). The amount of GCN20 in each fraction was determined as described for Fig. 9 except that 50 μl of each fraction was analyzed for the *GCN1* extracts, but 400 μl of each fraction was TCA precipitated and analyzed for the *gcn1*Δ extracts, because GCN20 is less abundant in *gcn1* mutants (47). For the same reason, a longer exposure of the immunoblot is shown for the *gcn1*Δ strain than for the *GCN1* strain. (B) Effect of the *gcn1-502* allele. Total-cell extracts from strain F113 and an otherwise isogenic transformant of H2079 harboring *gcn1-502* on plasmid p2395 were prepared and analyzed exactly as described above.

decreased the proportion of GCN20 that cosedimented with polysomes (Fig. 12B).

We wished to determine whether the ATP stimulation of ribosome binding by GCN1 and GCN20 was dependent on the ABC domains in GCN20. To answer this question, we examined the effect of deleting *GCN20* on ribosome binding by GCN1. In accord with the results in Fig. 11, the majority of GCN1 sedimented with polysomes when wild-type *GCN20* extracts were analyzed in the presence of ATP (Fig. 13A, GCN1 panels). In *gcn20*Δ extracts, the level of GCN1 binding to polysomes was increased in the absence of ATP and decreased in the presence of ATP relative to that seen in the wild-type extracts (compare GCN1 panels in Fig. 13B with those in Fig. 13A). In repetitions of this last experiment, we often observed residual ATP stimulation of polysome binding by GCN1 in *gcn20*Δ extracts (data not shown). We conclude that GCN1 can bind to ribosomes independently of GCN20; however, its interaction with ribosomes is relatively insensitive to ATP levels in the absence of GCN20.

We attempted to inactivate the ABCs in GCN20 by introducing point mutations at conserved positions in both cassettes, replacing Gly-371 and Gly-654 with aspartates. Each of these Gly residues is at the third position of the conserved (L/F)SGG motif located 20 residues N terminal to the Walker B motif ([I/L]L[L/V]LDE) in the predicted ABCs of GCN20 (47). Substitutions of the corresponding Gly residues in the cystic fibrosis gene product CFTR (9) and the yeast *a*-factor transporter STE6 (5) appeared to inactivate transporter function. It has been suggested that this motif is located in a loop region that functions in coupling ATP hydrolysis to transporter function (23). Similar to what was seen for the *GCN20* deletion alleles shown in Fig. 2 which lack both ABCs, the *GCN20-G371D,G654D* allele complemented the 3-AT^s phenotype of a *gcn20*Δ mutant indistinguishably from wild-type *GCN20* (data not shown). Thus, the point mutations in the putative ABCs did not reduce *GCN20*

regulatory function in histidine-starved cells. They did have a large effect on ribosome binding by GCN20, however, greatly diminishing its polysome association in the presence or absence of ATP (Fig. 13A and C, GCN20 panels). The *GCN20-G371D,G654D* mutation also greatly reduced, but did not abolish, binding of GCN1 to polysomes in the presence of ATP, with the majority of GCN1 remaining at the top of the gradients in both the presence and absence of ATP (Fig. 13A and C, GCN1 panels). Similar results were obtained with the strain expressing the truncated mutant form of GCN20 (encoded by p1739) which lacks both ABCs (data not shown). Thus, in the absence of the GCN20 ABCs, GCN20 shows little or no ribosome binding, whereas GCN1 retains the ability to interact with ribosomes, but does so in a manner that is relatively insensitive to ATP. Inactivation of the GCN20 ABCs did not impair derepression of *GCN4* translation in vivo. Therefore, the stable binding of a large fraction of GCN1 to polysomes in the presence of ATP seen in vitro, which depends on the ABCs, cannot be essential for activation of GCN2 in histidine-starved cells.

Finally, we investigated the possibility that histidine starvation might alter the fraction of GCN1 or GCN20 found associated with polysomes. The wild-type strain was grown in minimal medium as described above or in the presence of 3-AT to elicit histidine starvation, and the association of GCN1 and GCN20 with polysomes in cell extracts was analyzed in the presence or absence of ATP. The addition of 3-AT to the growth medium led to a reduction in the average size and amount of polysomes (data not shown), presumably reflecting phosphorylation of eIF2α by GCN2 and attendant inhibition of general translation initiation. The presence of 3-AT in the culture medium shifted the distribution of ribosome-associated GCN1 from large polysomes to smaller polysomes and 80S ribosomes, whether or not ATP was added to the extracts (Fig. 14). This shift in the size distribution of GCN1 roughly coincided with the effects of 3-AT on the total polysome profile

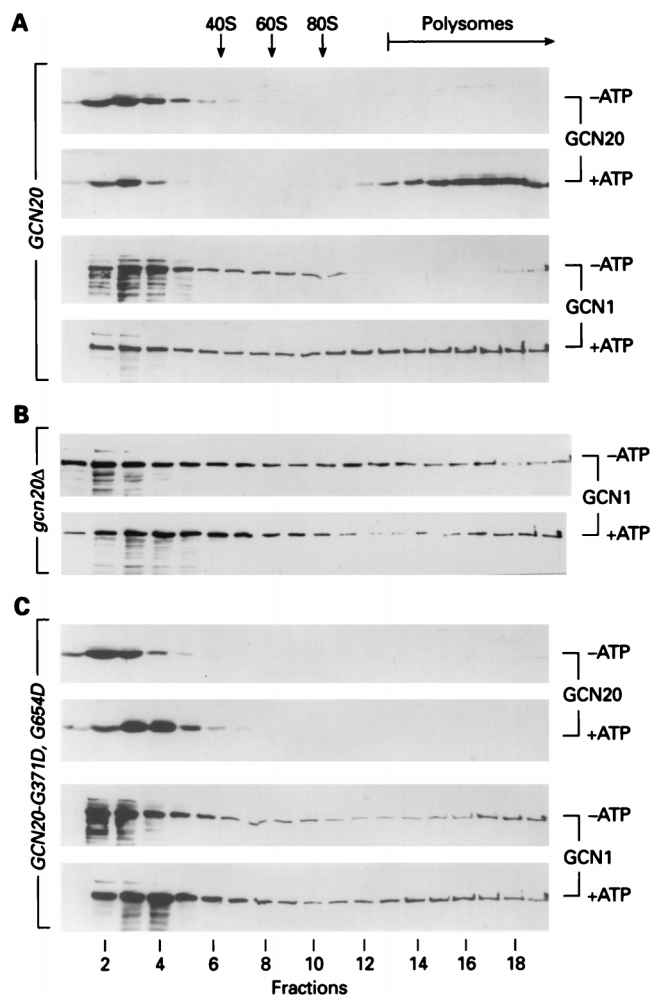


FIG. 13. ATP-stimulated polysome association of GCN20 and GCN1 is reduced by *gcn20* mutations. The *gcn20* Δ strain ED1001 was transformed with p1728 bearing wild-type *GCN20* (A), empty vector pRS316 (B), or p2343 bearing *GCN20-G371D,G654D* (C). Whole-cell extracts were prepared and fractionated by velocity sedimentation in sucrose density gradients in the presence or absence of ATP (indicated to the right) as described for Fig. 11. Arrows at the top indicate the positions of 40S and 60S subunits, 80S ribosomes, and polysomes, as determined from the UV absorbance profiles of the gradients (data not shown), and the numbers at the bottom panel indicate the gradient fractions from top to bottom. The amount of GCN1 or GCN20 (indicated to the right) present in each fraction was determined exactly as described for Fig. 9.

(data not shown). However, the fraction of GCN1 associated with ribosomes was not substantially altered by 3-AT treatment of the cultures (Fig. 14); consequently, there was no strong indication that the association of GCN1 with translating ribosomes was substantially altered by amino acid starvation. Similar results were obtained for GCN20 in the same extracts (data not shown).

DISCUSSION

Evidence that GCN1 and GCN20 function on ribosomes in activating GCN2 kinase function. GCN1 and GCN20 are required for activation of the protein kinase GCN2 by uncharged tRNA in amino acid-starved cells. In their absence, eIF2 is not phosphorylated by GCN2 at levels high enough to induce *GCN4* translation and the attendant transcriptional activation of amino acid biosynthetic genes under GCN4 control. GCN20

contains two putative ATP-binding domains characteristic of ABC transporters. Based on this similarity, we considered the possibility that GCN1 and GCN20 constitute an amino acid transporter that regulates GCN2 indirectly by influencing the levels of uncharged tRNA in the cytoplasm. According to this model, the ATP-binding domains and the MSDs of the transporter would be separately encoded by *GCN20* and *GCN1*, respectively. This structural organization is not uncommon for prokaryotic ABC transporters; however, for most eukaryotic ABC transporters, tandem duplications of the MSD-ABC units are fused in a single polypeptide chain (15). Moreover, the ABC domains in GCN20 are more similar to those found in EF3 than to the ABCs in any known membrane transporter. GCN1 is also similar to EF3 in a region located N terminal to the ABC domains in EF3, and it is difficult to rationalize this sequence similarity with a transporter model. These last considerations prompted a different hypothesis in which GCN1 and GCN20 would function more directly to activate GCN2, in a manner related to the role of EF3 in translation elongation. In this alternative model, the GCN1/GCN20 complex interacts with ribosomes and facilitates delivery of uncharged tRNA bound to the ribosomal A site to the synthetase-related domain in GCN2.

We found that GCN1 was localized throughout the cytoplasm and showed no obvious association with plasma or vacuolar membranes, contrary to the idea that it functions as the transmembrane component of an ABC transporter. In addition, the ABCs in GCN20 were found to be dispensable for its regulatory function in histidine-starved cells. Because the ABCs provide the energy coupling in ABC transporters for movement of substrates against a concentration gradient (23), this finding makes it unlikely that GCN1/GCN20 is an amino

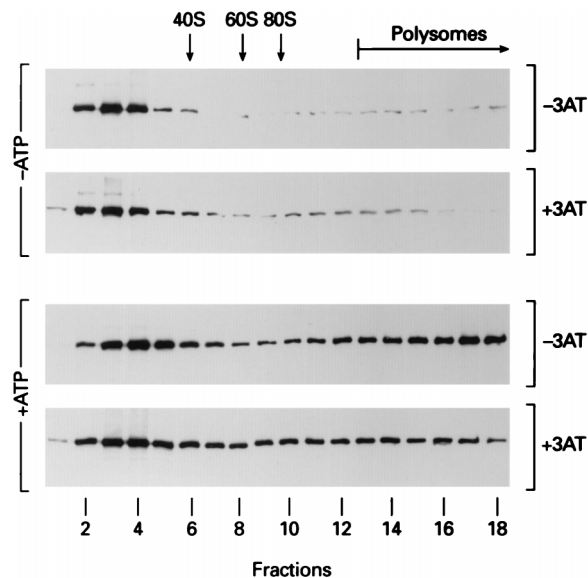


FIG. 14. Effects of histidine starvation on the polysome association of GCN1. A transformant of *gcn20* Δ strain ED1001 containing the *GCN20* plasmid p1728 was grown in SD medium for 15 h to an OD_{600} of ≈ 1.1 (-3AT) or for 13 h to an OD_{600} of ≈ 0.71 , after which 3-AT was added to 10 mM and growth was continued for another 2 h to an OD_{600} of ≈ 1.0 (+3AT). Whole-cell extracts were prepared and fractionated by velocity sedimentation in sucrose density gradients in the presence or absence of ATP (indicated to the left) as described for Fig. 11. Arrows at the top indicate the positions of 40S and 60S subunits, 80S ribosomes, and polysomes, as determined from the UV absorbance profiles of the gradients (data not shown), and the numbers at the bottom indicate the gradient fractions from top to bottom. The amounts of GCN1 present in each fraction were determined exactly as described for Fig. 9.

acid transporter. The N-terminal portion of GCN20 required for its regulatory function was found to be necessary and sufficient for complex formation with GCN1, and GCN20 bound to GCN1 in the region most highly related to EF3. This finding, plus the fact that the EF3-like region is the most highly conserved segment between GCN1 and the human homolog *H.s.GCN1* supports the notion that an important aspect of *GCN1* function is related to the activity of EF3 in translation elongation.

Physical evidence consistent with the notion that GCN1 and GCN20 function on ribosomes came from the finding that a proportion of GCN1 and GCN20 cosedimented with polysomes and 80S ribosomes. Ribosome binding by both proteins was stimulated by addition of ATP to the gradients, and under these conditions, it was evident that the interaction of GCN20 with polysomes was strongly dependent on GCN1 and on the ABCs in GCN20 itself. It was found that GCN1 could bind to polysomes in the absence of GCN20; however, the stimulatory effect of ATP on polysome binding by GCN1 was largely dependent on the GCN20 ABCs. These findings suggest that the energy of ATP hydrolysis leads to a conformational change in the GCN1/GCN20 complex that promotes a stable interaction with translating ribosomes. The nonhydrolyzable ATP analog AMP-PNP did not mimic ATP in promoting high-level binding of GCN1 and GCN20 to polysomes. This could indicate that ATP hydrolysis is required for the conformational change that promotes stable ribosome binding by GCN1/GCN20. The fact that a low level of ATP stimulation of ribosome binding by GCN1 occurred in *gcn20* mutants could indicate that GCN1 can interact with another ABC protein, e.g., the GCN20 homolog ORF YER036c, that will stimulate its interaction with ribosomes in the absence of functional ABCs in GCN20.

We found that GCN1 and GCN20 were not distributed identically throughout the monosome and polysome fractions. This finding is consistent with the fact that GCN1, and to a lesser extent GCN20, can interact with polysomes in the absence of the other protein. Thus, each seems to possess an intrinsic affinity for ribosomes that is increased by complex formation between the two proteins. It is possible that the interaction between GCN1 and GCN20 is more dynamic than previously imagined and that dissociation of the complex occurs more readily when the complex is bound to ribosomes or is subjected to the sedimentation force. Another contributing factor could be that roughly one-fourth of GCN20 does not appear to be complexed with GCN1 in the cell, and this proportion may be even greater in whole-cell extracts (47).

A model for the role of GCN1/GCN20 in the activation of GCN2 on translating ribosomes. It has been shown that GCN2 interacts with ribosomes, prompting the suggestion that activation of GCN2 by uncharged tRNA occurs on translating ribosomes (35). In accord with previous observations (47), we found that ribosome binding by GCN2 was unaffected by mutations in *GCN1* or *GCN20* or by addition of ATP to the gradients (data not shown). Thus, the GCN1/GCN20 complex does not appear to function by recruiting GCN2 to ribosomes. We obtained no evidence that ribosome binding by GCN1 or GCN20 is stimulated under amino acid starvation conditions; however, it is possible that such stimulation occurs *in vivo* but is not maintained in the cell extracts. The facts that the EF3-like region of GCN1 is highly conserved in the homologous human protein *H.s.GCN1* and that the critical N-terminal segment of GCN20 binds to the EF3-like region in GCN1 both suggest that some aspect of GCN1 function is related to the activity of EF3 in translation elongation. Biochemical analysis indicates that EF3 promotes a conformational change in the ribosome that results in release of deacylated tRNA from the

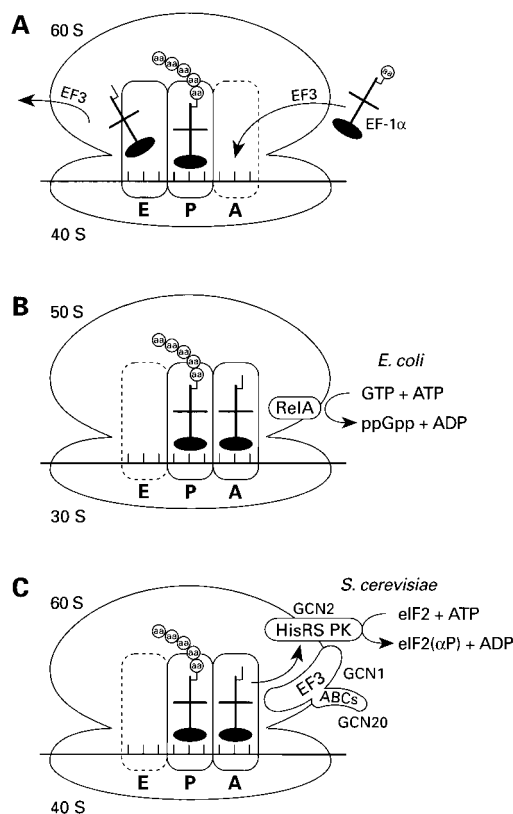


FIG. 15. A model describing an EF3-related function of GCN1 and GCN20 on translating ribosomes in activation of protein kinase GCN2 by uncharged tRNA. (A) Right arrow, EF3 stimulates binding of cognate aminoacyl-tRNA/GTP/EF1 α complexes to the ribosomal A site at the expense of noncognate tRNA binding, consistent with its proposed role in translational fidelity. Left arrow, EF3 stimulates release of deacylated tRNA from the ribosomal E site. (B) In *E. coli*, limitation for an amino acid results in accumulation of uncharged tRNA in the cytosol. RelA interacts with ribosomes in the vicinity of the A site, and binding of uncharged tRNA to the A site stimulates the production of ppGpp by RelA. Increased levels of ppGpp trigger the stringent response. RelA may also promote binding of uncharged tRNA to the A site. (C) Proposed mechanism for activation of GCN2 by GCN1 and GCN20 on translating ribosomes. GCN2 is a ribosome-associated eIF2 α protein kinase (PK) with a histidyl-tRNA-synthetase (HisRS) domain that binds tRNA *in vitro* and is required for kinase activation by uncharged tRNA in amino acid-starved cells. GCN1 and GCN20 stimulate GCN2 kinase activity in response to amino acid limitation. By analogy with RelA in bacteria, and considering the importance of the EF3-like region in GCN1, we propose that the GCN1/GCN20 complex binds near the A site and functions in an EF3-like manner to stimulate the binding of uncharged tRNA to the A site or its delivery to the HisRS-like domain in GCN2. The ABCs in GCN20 may modulate GCN1 activity when cells are energy starved or depleted of nutrients besides amino acids.

ribosomal E site and binding of EF-1 α /GTP/aminoacyl-tRNA ternary complexes to the A site in each round of translation elongation (45) (Fig. 15A). It may also function in promoting the fidelity of codon-anticodon pairing by the incoming aminoacylated tRNA at the A site (46). Thus, it is tempting to propose that GCN1 functions on the ribosome in an EF3-like manner to facilitate activation of GCN2 by uncharged tRNA.

In *E. coli*, the RelA protein is associated with the A site in a small fraction of ribosomes and stimulates production of guanosine tetraphosphate (ppGpp) from ATP and GTP in response to binding of uncharged tRNA (8). The production of ppGpp in amino acid-starved *E. coli* cells leads to derepression of amino acid biosynthetic genes and, in this sense, is analogous to the GCN4-dependent derepression of amino acid bio-

synthetic genes elicited by phosphorylation of eIF2 α in amino acid-starved yeast cells (Fig. 15B and C). There is in vitro evidence that RelA directs the binding of uncharged tRNA to the A site rather than the P site and that hydrolysis of ATP by RelA subsequently promotes release of the tRNA (36). By analogy with the function of RelA, the GCN1/GCN20 complex may promote binding of uncharged tRNA to the A site in amino acid-starved cells or promote the transfer of uncharged tRNA from the A site to the GCN2 HisRS-like domain (Fig. 15C). These functions could be analogous to the role of EF3 in removing deacylated tRNA from the E site. The coupling of GCN2 activation with the codon-specific binding and release of uncharged tRNA at the A site would ensure that GCN2 is activated efficiently even when the cognate tRNAs for only a single amino acid are not fully charged.

GCN1 is most highly related to the segment of EF3 located N terminal to the ABCs. Little is known about the function of this domain, making it difficult to predict whether GCN1 mimics the ribosome-binding activity of EF3 or some aspect of its catalytic function. It is interesting, however, that this region overlaps a segment with similarity to a portion of bacterial ribosomal protein S5, leading to the suggestion that EF3 is the eukaryotic equivalent of the S4-S5-S12 ribosomal accuracy center (4). It was also suggested that EF3 and GCN1 contain hydrophobic residues at positions which comprise the hydrophobic core in S5, perhaps indicating that all three proteins are structurally related. These observations raise the intriguing possibility that the proposed function of GCN1 in promoting binding or release of uncharged tRNA at the A site is analogous to the A-site function of S5 in promoting recognition of cognate aminoacyl-tRNAs.

The N-terminal 15 to 25% of GCN20 is the only part of the protein essential for its ability to cooperate with GCN1 in mediating activation of GCN2 in histidine-starved cells. By contrast, at least 90% of the 2,672 amino acids in GCN1 are required for its ability to activate GCN2 under the same conditions. In addition, deletion of *GCN1* impairs GCN2 kinase activity in vivo more completely than does deletion of *GCN20* (31, 47). From these findings, it appears that GCN1 is more critically required than GCN20 for activation of GCN2 by uncharged tRNA. Although interaction of the N-terminal segment of GCN20 with the EF3-like domain in GCN1 is essential for the ability of GCN1 to mediate activation of GCN2, perhaps this interaction arose primarily to provide a means of modulating GCN1 function. If so, the ABCs in GCN20 may be involved in this regulatory function. It has been proposed that hydrolysis of ATP induces a conformational change in ABC transporters that mediates movement of substrates across the membrane (18, 23). By analogy with this model, it could be imagined that hydrolysis of ATP by GCN20 elicits a conformational change in the GCN1/GCN20 complex that alters its interaction with ribosomes or its ability to activate GCN2 in the manner depicted in Fig. 15.

Because the GCN20 ABCs were largely dispensable for activation of GCN2 in histidine-starved cells, the stimulatory effect of ATP on ribosome binding that we observed in vitro does not appear to be required for efficient activation of GCN2 under these starvation conditions. To explain this apparent anomaly, it could be proposed that the GCN1/GCN20 complex cycles continuously between ribosome-associated (ATP-bound) and ribosome-free (ADP-bound) forms. In a *GCN20* mutant lacking the ABCs, GCN1 would no longer cycle on and off the ribosome; however, it might still achieve a constitutive level of ribosome binding similar to that which occurs in wild-type cells under the histidine starvation conditions of our experiments. The elevated level of ribosome binding by GCN1/

GCN20 seen upon addition of ATP to the extracts might be required to achieve an even higher level of GCN2 activation under starvation conditions that are more severe than those imposed here. Alternatively, it may be required under different starvation or stress conditions where amino acids are abundant and uncharged tRNAs would not be expected to accumulate, e.g., carbon starvation or heat shock. Activation of GCN2 might occur with the low basal levels of uncharged tRNA present under these latter conditions simply by an increase in the ribosomal occupancy of the GCN1/GCN20 complex.

Alternatively, it is possible that the ABCs function to down-regulate GCN1/GCN20 binding to ribosomes under conditions of carbon or energy starvation where ATP/ADP ratios are low and the induction of amino acid biosynthetic genes might be unproductive. A low ATP/ADP ratio present in energy-starved cells would cause the ADP-bound form of GCN1 and GCN20 to predominate, preventing ribosome association of the complex and thereby blocking activation of GCN2. Because the ABCs would function to prevent GCN2 activation in energy-deprived cells, their removal would have no effect on *GCN4* expression in energy-replete, amino acid-starved cells. This model is prompted by recent observations on the role of the sulfonyleurea receptor in coupling the activity of the pancreatic potassium channel to blood glucose concentration and intracellular ATP/ADP ratios (33).

There are other ways to explain why removing the GCN20 ABCs fails to reduce *GCN4* expression, including the possibility that the GCN20 homolog encoded by ORF YER036c can functionally compensate for the absence of GCN20 ABCs and restore activation of GCN2. It is also possible that the ABCs in GCN20 are required for some other ribosomal function of the GCN1/GCN20 complex unrelated to activation of GCN2 in amino acid-starved cells. To distinguish between these different models, it will be necessary to mutate the ABC domains in GCN20 individually and in combination, both in the presence and in the absence of the ORF YER036c product, and measure the effects of these mutations on *GCN4* expression under different starvation and stress conditions.

ACKNOWLEDGMENTS

We thank Diego Loayza and Susan Michaelis for advice and assistance in the localization of GCN1, Minerva Garcia for advice on sucrose gradient fractionations and immunoblotting, Jim Anderson for the PUB2 antibody, and Shauna Everett in the NIH Photomicroscopy group for help on preparing immunofluorescence images. We thank Tom Dever and Graham Pavitt for comments on the manuscript and Bobbie Felix for assistance in its preparation.

REFERENCES

- Alani, E., L. Cao, and N. Kleckner. 1987. A method for gene disruption that allows repeated use of *URA3* selection in the construction of multiply disrupted yeast strains. *Genetics* **116**:541-545.
- Altschul, S. F., W. Gish, W. Miller, E. W. Myers, and D. J. Lipman. 1990. Basic local alignment search tool. *J. Mol. Biol.* **215**:403-410.
- Anderson, J. T., M. R. Paddy, and M. S. Swanson. 1993. PUB1 is a major nuclear and cytoplasmic polyadenylated RNA-binding protein in *Saccharomyces cerevisiae*. *Mol. Cell. Biol.* **13**:6102-6113.
- Belfield, G. P., N. J. Ross-Smith, and M. F. Tuite. 1995. Translation elongation factor-3 (EF-3): an evolving eukaryotic ribosomal protein. *J. Mol. Evol.* **41**:376-387.
- Berkower, C., and S. Michaelis. 1991. Mutational analysis of the yeast a-factor transporter STE6, a member of the ATP binding cassette (ABC) protein superfamily. *EMBO J.* **10**:3777-3785.
- Boeke, J. D., F. LaCroute, and G. R. Fink. 1984. A positive selection for mutants lacking orotidine-5'-phosphate decarboxylase activity in yeast: 5-fluoro-orotic acid resistance. *Mol. Gen. Genet.* **197**:345-346.
- Boguski, M. S., and F. McCormick. 1993. Proteins regulating Ras and its relatives. *Nature* **366**:643-654.
- Cashel, M., and K. E. Rudd. 1987. The stringent response, p. 1410-1438. *In* F. C. Neidhardt, J. L. Ingraham, K. B. Low, B. Magasanik, M. Schaechter,

- and H. E. Umbarger (ed.), *Escherichia coli* and *Salmonella typhimurium*: cellular and molecular biology. American Society for Microbiology, Washington, D.C.
9. Cutting, G. R., L. M. Kasch, B. J. Rosentein, J. Zielenski, L.-C. Tsui, S. E. Antonarakis, and H. Kazazian. 1990. A cluster of cystic fibrosis mutations in the first nucleotide-binding fold of the cystic fibrosis conductance regulator protein. *Nature* **346**:366–369.
 10. Dasmahapatra, B., and K. Chakraburty. 1981. Protein synthesis in yeast. I. Purification and properties of elongation factor 3 from *Saccharomyces cerevisiae*. *J. Biol. Chem.* **256**:9999–10004.
 11. Dever, T. E., L. Feng, R. C. Wek, A. M. Cigan, T. D. Donahue, and A. G. Hinnebusch. 1992. Phosphorylation of initiation factor 2 α by protein kinase GCN2 mediates gene-specific translational control of *GCN4* in yeast. *Cell* **68**:585–596.
 12. Devereux, J., P. Haerberli, and O. Smithies. 1984. A comprehensive set of sequence analysis programs for the VAX. *Nucleic Acids Res.* **12**:387–395.
 13. Donahue, T. F., R. S. Daves, G. Lucchini, and G. R. Fink. 1983. A short nucleotide sequence required for regulation of *HIS4* by the general control system of yeast. *Cell* **32**:89–98.
 14. Durfee, T., K. Becherer, P. L. Chen, S. H. Yeh, Y. Yang, A. E. Kilburn, W. H. Lee, and S. J. Elledge. 1993. The retinoblastoma protein associates with the protein phosphatase type 1 catalytic subunit. *Genes Dev.* **7**:555–569.
 15. Fath, M. J., and R. Kolter. 1993. ABC transporters: bacterial exporters. *Microbiol. Rev.* **57**:995–1017.
 16. Feilotter, H. E., G. J. Hannon, C. J. Ruddell, and D. Beach. 1994. Construction of an improved host strain for two hybrid screening. *Nucleic Acids Res.* **22**:1502–1503.
 17. Feinberg, B., C. S. McLaughlin, and K. Moldave. 1982. Analysis of temperature-sensitive mutant ts187 of *Saccharomyces cerevisiae* altered in a component required for the initiation of protein synthesis. *J. Biol. Chem.* **257**:10846–10851.
 18. Ferro-Luzzi Ames, G. 1992. Bacterial periplasmic permeases as model systems for the superfamily of traffic ATPases, including the multidrug resistance protein and the cystic fibrosis transmembrane conductance regulator. *Int. Rev. Cytol.* **137A**:1–35.
 19. Foiani, M., A. M. Cigan, C. J. Paddon, S. Harashima, and A. G. Hinnebusch. 1991. GCD2, a translational repressor of the *GCN4* gene, has a general function in the initiation of protein synthesis in *Saccharomyces cerevisiae*. *Mol. Cell. Biol.* **11**:3203–3216.
 20. Gietz, R. D., and A. Sugino. 1988. New yeast-*Escherichia coli* shuttle vectors constructed with in vitro mutagenized yeast genes lacking six-base pair restriction sites. *Gene* **74**:527–34.
 21. Hannig, E. H., N. P. Williams, R. C. Wek, and A. G. Hinnebusch. 1990. The translational activator GCN3 functions downstream from GCN1 and GCN2 in the regulatory pathway that couples *GCN4* expression to amino acid availability in *Saccharomyces cerevisiae*. *Genetics* **126**:549–562.
 22. Hershey, J. W. B. 1991. Translational control in mammalian cells. *Annu. Rev. Biochem.* **60**:717–755.
 23. Higgins, C. F. 1992. ABC transporters: from microorganisms to man. *Annu. Rev. Cell Biol.* **8**:67–113.
 24. Hinnebusch, A. G. 1996. Translational control of *GCN4*: gene-specific regulation by phosphorylation of eIF2, p. 199–244. In J. W. B. Hershey, M. B. Mathews, and N. Sonenberg (ed.), *Translational control*. Cold Spring Harbor Laboratory Press, Cold Spring Harbor, N.Y.
 25. Kamath, A., and K. Chakraburty. 1989. Role of yeast elongation factor 3 in the elongation cycle. *J. Biol. Chem.* **264**:15423–15428.
 26. Kane, P. M., M. C. Kuehn, I. Howald-Stevenson, and T. H. Stevens. 1992. Assembly and targeting of peripheral and integral membrane subunits of the yeast vacuolar H⁺-ATPase. *J. Biol. Chem.* **267**:447–454.
 27. Klionsky, D. J., P. Herman, and S. D. Emr. 1990. The fungal vacuole: composition, function, and biogenesis. *Microbiol. Rev.* **54**:266–292.
 28. Koerner, T. J., J. E. Hill, A. M. Myers, and A. Tzagoloff. 1991. High-expression vectors with multiple cloning sites for construction of *trpE* fusion genes: pATH vectors. *Methods Enzymol.* **194**:477–490.
 29. Lanker, S., J. L. Bushman, A. G. Hinnebusch, H. Trachsel, and P. P. Mueller. 1992. Autoregulation of the yeast lysyl-tRNA synthetase gene *GCD5/KRS1* by translational and transcriptional control mechanisms. *Cell* **70**:647–657.
 30. Lennon, G., C. Auffray, M. Polymeropoulos, and M. B. Soares. 1996. The I.M.A.G.E. consortium: an integrated molecular analysis of genomes and their expression. *Genomics* **33**:151–152.
 31. Marton, M. J., D. Crouch, and A. G. Hinnebusch. 1993. GCN1, a translational activator of *GCN4* in *Saccharomyces cerevisiae*, is required for phosphorylation of eukaryotic translation initiation factor 2 by protein kinase GCN2. *Mol. Cell. Biol.* **13**:3541–3556.
 - 31a. Marton, M. J., and A. G. Hinnebusch. Unpublished data.
 32. Naranda, T., S. E. MacMillan, and J. W. B. Hershey. 1994. Purified yeast translational initiation factor eIF-3 is an RNA-binding protein complex that contains the PRT1 protein. *J. Biol. Chem.* **269**:32286–32292.
 33. Nichols, C. G., S.-L. Shyng, A. Nestorowicz, B. Glaser, J. P. Clement, G. Gonzalez, L. Aguilar-Bryan, M. A. Permutt, and J. Bryan. 1996. Adenosine diphosphate as an intracellular regulator of insulin secretion. *Science* **272**:1785–1787.
 34. Petitjean, A., N. Bonneaud, and F. Lacroute. 1995. The duplicated *Saccharomyces cerevisiae* gene *SSM1* encodes a eucaryotic homolog of the eubacterial and archaeobacterial L1 ribosomal proteins. *Mol. Cell. Biol.* **15**:5071–5081.
 35. Ramirez, M., R. C. Wek, and A. G. Hinnebusch. 1991. Ribosome-association of GCN2 protein kinase, a translational activator of the *GCN4* gene of *Saccharomyces cerevisiae*. *Mol. Cell. Biol.* **11**:3027–3036.
 36. Richter, D. 1976. Stringent factor from *Escherichia coli* directs ribosomal binding and release of uncharged tRNA. *Proc. Natl. Acad. Sci. USA* **73**:707–711.
 37. Roberts, C. J., C. K. Raymond, C. T. Yamashiro, and T. H. Stevens. 1991. Methods for studying the yeast vacuole. *Methods Enzymol.* **194**:644–661.
 38. Rolfes, R. J., F. Zhang, and A. G. Hinnebusch. 1997. The transcriptional activators BAS1, BAS2, and ABF1 bind positive regulatory sites as the critical elements for adenine regulation of *ADE5,7*. *J. Biol. Chem.* **272**:13343–13354.
 39. Sandbaken, M., J. A. Lupisella, B. DiDomenico, and K. Chakraburty. 1990. Isolation and characterization of the structural gene encoding elongation factor 3. *Biochim. Biophys. Acta* **1050**:230–234.
 40. Sato, T., Y. Ohsumi, and Y. Anraku. 1984. An arginine/histidine exchange transport system in vacuolar-membrane vesicles of *Saccharomyces cerevisiae*. *J. Biol. Chem.* **259**:11509–11511.
 41. Sato, T., Y. Ohsumi, and Y. Anraku. 1984. Substrate specificities of active transport systems for amino acids in vacuolar-membrane vesicles of *Saccharomyces cerevisiae*. *J. Biol. Chem.* **259**:11505–11508.
 42. Sikorski, R. S., and P. Hieter. 1989. A system of shuttle vectors and yeast host strains designed for efficient manipulation of DNA in *Saccharomyces cerevisiae*. *Genetics* **122**:19–27.
 43. Skogerson, L., and E. Wakatama. 1976. A ribosome-dependent GTPase from yeast distinct from elongation factor 2. *Proc. Natl. Acad. Sci. USA* **73**:73–76.
 44. Szczypka, M. S., J. A. Wemmie, W. S. Moye-Rowley, and D. J. Thiele. 1994. A yeast metal resistance protein similar to human cystic fibrosis transmembrane conductance regulator (CFTR) and multidrug resistance-associated protein. *J. Biol. Chem.* **269**:22853–22857.
 45. Triana-Alonso, F. J., K. Chakraburty, and K. H. Nierhaus. 1995. The elongation factor unique in higher fungi and essential for protein biosynthesis is an E site factor. *J. Biol. Chem.* **270**:20473–20478.
 46. Uritani, M., and M. Miyazaki. 1988. Role of yeast elongation factor 3 (EF-3) at the AA-tRNA binding step. *J. Biochem.* **104**:118–126.
 47. Vazquez de Aldana, C. R., M. J. Marton, and A. G. Hinnebusch. 1995. GCN20, a novel ATP binding cassette protein, and GCN1 reside in a complex that mediates activation of the eIF-2 α kinase GCN2 in amino acid-starved cells. *EMBO J.* **14**:3184–3199.
 48. Wek, R. C., B. M. Jackson, and A. G. Hinnebusch. 1989. Juxtaposition of domains homologous to protein kinases and histidyl-tRNA synthetases in GCN2 protein suggests a mechanism for coupling *GCN4* expression to amino acid availability. *Proc. Natl. Acad. Sci. USA* **86**:4579–4583.
 49. Wek, S. A., S. Zhu, and R. C. Wek. 1995. The histidyl-tRNA synthetase-related sequence in the eIF-2 α protein kinase GCN2 interacts with tRNA and is required for activation in response to starvation for different amino acids. *Mol. Cell. Biol.* **15**:4497–4506.
 50. Wemmie, J. A., M. S. Szczypka, D. J. Thiele, and W. S. Moye-Rowley. 1994. Cadmium tolerance mediated by the yeast AP-1 protein requires the presence of an ATP-binding cassette transporter-encoding gene, *YCF1*. *J. Biol. Chem.* **269**:32592–32597.
 51. Wiemkin, A., M. Schellenberg, and K. Urech. 1979. Vacuoles: the sole compartments of digestive enzymes in yeast *Saccharomyces cerevisiae*? *Arch. Microbiol.* **123**:23–35.
 52. Yamashiro, C. T., P. M. Kane, D. F. Wolczyk, R. A. Preston, and T. H. Stevens. 1990. Role of vacuolar acidification in protein sorting and zymogen activation: a genetic analysis of the yeast vacuolar proton-translocating ATPase. *Mol. Cell. Biol.* **10**:3737–3749.
 53. Yon, J., and M. Fried. 1988. Precise gene fusion by PCR. *Nucleic Acids Res.* **17**:4895.